

University of Nevada, Reno

**Carlin-Type Mineralization and Alteration of Late Cambrian and Ordovician
Carbonate Rocks at Long Canyon, Pequop Mountains, Nevada**

A thesis submitted in partial fulfillment of the
requirements for the degree of Master of Science in
Geology

by

Zachary J. Jarvie

Dr. Tommy B. Thompson/Thesis Advisor

December, 2009

UMI Number: 1478542

All rights reserved

INFORMATION TO ALL USERS

The quality of this reproduction is dependent upon the quality of the copy submitted.

In the unlikely event that the author did not send a complete manuscript and there are missing pages, these will be noted. Also, if material had to be removed, a note will indicate the deletion.



UMI 1478542

Copyright 2010 by ProQuest LLC.

All rights reserved. This edition of the work is protected against unauthorized copying under Title 17, United States Code.



ProQuest LLC
789 East Eisenhower Parkway
P.O. Box 1346
Ann Arbor, MI 48106-1346



University of Nevada, Reno
Statewide • Worldwide

THE GRADUATE SCHOOL

We recommend that the thesis
prepared under our supervision by

ZACHARY JARVIE

entitled

**Carlin-Type Mineralization and Alteration of Late Cambrian and Ordovician
Carbonate Rocks at Long Canyon, Pequop Mountains, Nevada**

be accepted in partial fulfillment of the
requirements for the degree of

MASTER OF SCIENCE

Dr. Tommy B. Thompson, Advisor

Dr. Jonathon G. Price, Committee Member

Dr. Victor R. Vasquez, Graduate School Representative

Marsha H. Read, Ph. D., Associate Dean, Graduate School

December, 2009

Abstract

This study examines local carbonate-hosted disseminated gold deposits near Long Canyon in the northern part of the Pequop Mountains located in northeastern Nevada. Several features typical of Carlin-type mineralization can be observed at the Long Canyon prospect. Gold is primarily hosted in Cambro-Ordovician limestone units, with mineralization commonly focused along structural features such as the lithologic contacts between the Cambrian Notch Peak limestone, the overlying Notch Peak dolostone and Ordovician aged Pogonip group limestone units. Like other Carlin-type deposits in Nevada, gold mineralization at Long Canyon is strongly associated with decarbonatization and silicification of carbonate host rocks. Geochemical and petrographic observations reveal silica introduction to be significant despite the fact that silicified limestones or jasperoids are volumetrically insignificant at Long Canyon. Rims of arsenian pyrite which are characteristic of Carlin-type deposits, around preexisting non-arsenian pyrite have been observed in the samples studied here. Typical of Carlin-type deposits, As, Fe, Si, Sb and Hg show a clear and strong chemical correlation to Au. Additionally, there is some evidence that elements Cd, Se, P, Sn, Tl, Be, Li, Pb, Ti, V, and Zr may also be associated with Au at Long Canyon. In high-grade samples, gold is commonly observed as discrete 2-5 μ m blebs of pure [native] gold. The deposits at Long Canyon are highly oxidized. Ore-grade material is strongly hematitic with locally observable jarosite and scorodite. Surviving gold-stage sulfide minerals such as arsenian pyrite are only observed where encapsulated in quartz. Despite the generally oxidizing conditions in the system, it is not uncommon for unmineralized samples to contain trace amounts of very fine diagenetic pyrite surviving due to encapsulation in both quartz and

calcite grains. Intrusive rocks are locally observable on the site as swarms of (or individual) dikes and sills. These can serve as a favorable host for gold mineralization; however, they appear to be volumetrically insignificant.

In loving dedication to

Mark and Kathryn Jarvie

It was a long but memorable drive from Michigan to Nevada.

Acknowledgements

Funding for this thesis was provided by

Center for Research in Economic Geology
Mackey School of Earth Sciences and Engineering
University of Nevada, Reno

New West Gold Inc.

Personal thanks to a number of geologists both in industry and at the university for impute, guidance, and assistance in all aspects of this project.

Specifically thanks are due to.

My advisory committee

Tommy B. Thompson
Jonathon G. Price
Victor R. Vasquez

Industry geologists

Bob Felder
Warren Thompson
Maira Smith

Special thanks also go to.

UNR professor

John McCormack, for training me on the XRD, assisting with SEM analysis, and for just being an all-around swell guy.

Table of Contents	page
Abstract	i
Dedication	iii
Acknowledgements	iv
Introduction	1
Previous Work	3
Stratigraphy	3
Structure	9
Methodologies and Data	11
Carbonate Alteration and Mineralization	16
Decarbonatization	16
Silicification	20
Gold and Sites of Gold	24
Fe Sulfide	28
Additional Sulfide Minerals	31
Fe Oxide	31
Illite and Sericite/Muscovite	35
Kaolinite	37
Other Minor Mineral Phases	38
Geochemistry	40
Intrusive Rocks	45
Alteration and Mineralization	49
Summary and Discussion of Igneous Rocks	50
Apatite	54
Discussion	57
Conclusions and Areas of Future Research	59
References Cited	61

Tables	page
---------------	-------------

Table 1. Selected chemical data for samples of Notch Peak limestone.	22
Table 2. Summary of kaolinite detections in XRD.	37
Table 3. Analytical results for unmineralized intrusive rocks collected at Long Canyon compared to typical whole rock oxide ranges for calc-alkaline, alkaline and ultra-mafic lamprophyres provided by Rock (1991, p. 41).	46
Table 4. Summary of apatite in sample set.	55

Figures	page
----------------	-------------

Figure 1. Location map of Long Canyon prospect.	2
Figure 2. Stratigraphic column of Long Canyon.	5
Figure 3. Decarbonatization effects on limestone host rocks vs. Au mineralization.	17
Figure 4. CaO and MgO values for samples Notch Peak dolomite vs. Au.	17
Figure 5. Sample LC07ZJ086.	18
Figure 6. Sample LC07ZJ083.	19
Figure 7. Jasperoid photomicrographs.	21
Figure 8. Silicification effects on limestone host rocks vs. Au.	23
Figure 9. LC07ZJ153 Gold bleb.	25
Figure 10. LC07ZJ153 SEM image of gold bleb in figure 9.	25
Figure 11. LC07ZJ126 gold bleb in decarbonatized limestone.	26
Figure 12. LC07ZJ126 SEM image of gold bleb in figure 11.	26
Figure 13. LC07ZJ156 Gold bleb on rim of hematite pseudomorph after pyrite.	27
Figure 14. LC07ZJ156 SEM image of 2 gold blebs on rim of hematite pseudomorph after pyrite.	27
Figure 15. LC07ZJ126 Pyrite (not arsenian) encapsulated in quartz.	29
Figure 16. LC07ZJ126 SEM image pyrite in figure 15.	29

Figures (continued)	page
Figure 17. SEM photo and EDS spectra of arsenian rim on pyrite, encapsulated in quartz found in sample LC07ZJ069.	30
Figure 18. Pictures of oxide relations as viewed macroscopically in thin section.	33
Figure 19. LC07ZJ126 Jarosite with hematite.	34
Figure 20. Joints that focus local (green) scoroditic alteration with hematite halos.	34
Figure 21. Au vs. K ₂ O.	36
Figure 22. Chondrite normalized plot diagram for rare earth elements in Long Canyon intrusive rocks.	46
Figure 23. LC08ZJ001: Platy biotite in matrix of albite and quartz.	51
Figure 24. LC07ZJ032: Platy biotite replaced by illite and hematite.	51
Figure 25. LC07ZJ082: calcite replacement of feldspar(?)phenocryst.	52
Figure 26. LC07ZJ082: same view as Figure 25, in reflected light.	52
Figure 27. LC07ZJ065: Hornblende with plagioclase (twinned).	53
Figure 28. LC07ZJ065: Hornblende altering to chlorite; Allanite (Ce) fan; Apatite needles in Oligoclase.	53
Figure 29. Photomicrographs of apatite.	56

Plates on CD

- Plate 1. Alteration at Long Canyon, Pequop Mountains Nevada
- Plate 2. Cross sections A-A' and B-B'
- Plate 3. Sample Location Map
- Plate 4. Exploration Geochemistry Sample Location Map
- Plate 5. Geochemical soil anomalies
 - 5 a. Au soil anomaly
 - 5 b. As soil anomaly
 - 5 c. Sb soil anomaly
 - 5 d. Hg soil anomaly

Appendices on CD

- A.1 Thin section descriptions with selected, annotated photomicrographs and a summary of XRD results (all photomicrographs are contained in Appendix A.2)
- A.2 Sample image files: outcrop and hand sample pictures, thin section photomicrographs (as referenced in Appendix A.1), SEM images, and XRD analyses
- B Analytical results for sample geochemistry
 - Table B.1 Whole rock oxide analysis
 - Table B.2 Assay and ICP analysis
- C Tables of correlation coefficients for chemical phases analyzed in samples collected for this study. (Includes statistical analysis of samples collected by the author. Statistical analysis of exploration rock, soil or drilling samples from Long canyon are not included.)
- D.1 Chemical plots vs. Au (for samples collected by the author)
- D.2 Chemical plots vs. Au for exploration soil grid samples
- D.3 Chemical plots vs. Au for surface rock exploration samples
- D.4 Chemical plots vs. Au for 2006 and 2007 drilling program samples

Introduction

The Pequop Mountains are located roughly 19 miles east of the town of Wells, Nevada along Interstate Highway 80. The Long Canyon mineralized zones examined in this study are located on the eastern slope of the Pequop Range immediately west and northwest of the Big Springs Ranch, which is located 4 ½ miles south of the Oasis exit (*Fig. 1*). At the time of the writing of this thesis, mineral exploration at Long Canyon is being performed by Fronteer Development USA Inc. (www.fronteergroup.com) in joint venture with AuEx Ventures Inc. (www.auexventures.com). Mineralization at Long Canyon is exposed at the surface via an erosional window that exposes the Cambrian Notch Peak limestones and dolostones that underlie the Ordovician Pogonip Group [sedimentary package]. Gold is hosted predominantly in limestone units, most commonly focused along the lithologic contacts between dolomite and surrounding Cambro-Ordovician limestone units and other associated structural features. It has been recognized from early exploration that Au mineralization at Long Canyon was most likely Carlin-type in nature. The purpose of this study is to characterize mineralization and alteration observed at the surface through visual, chemical, and petrographic techniques.

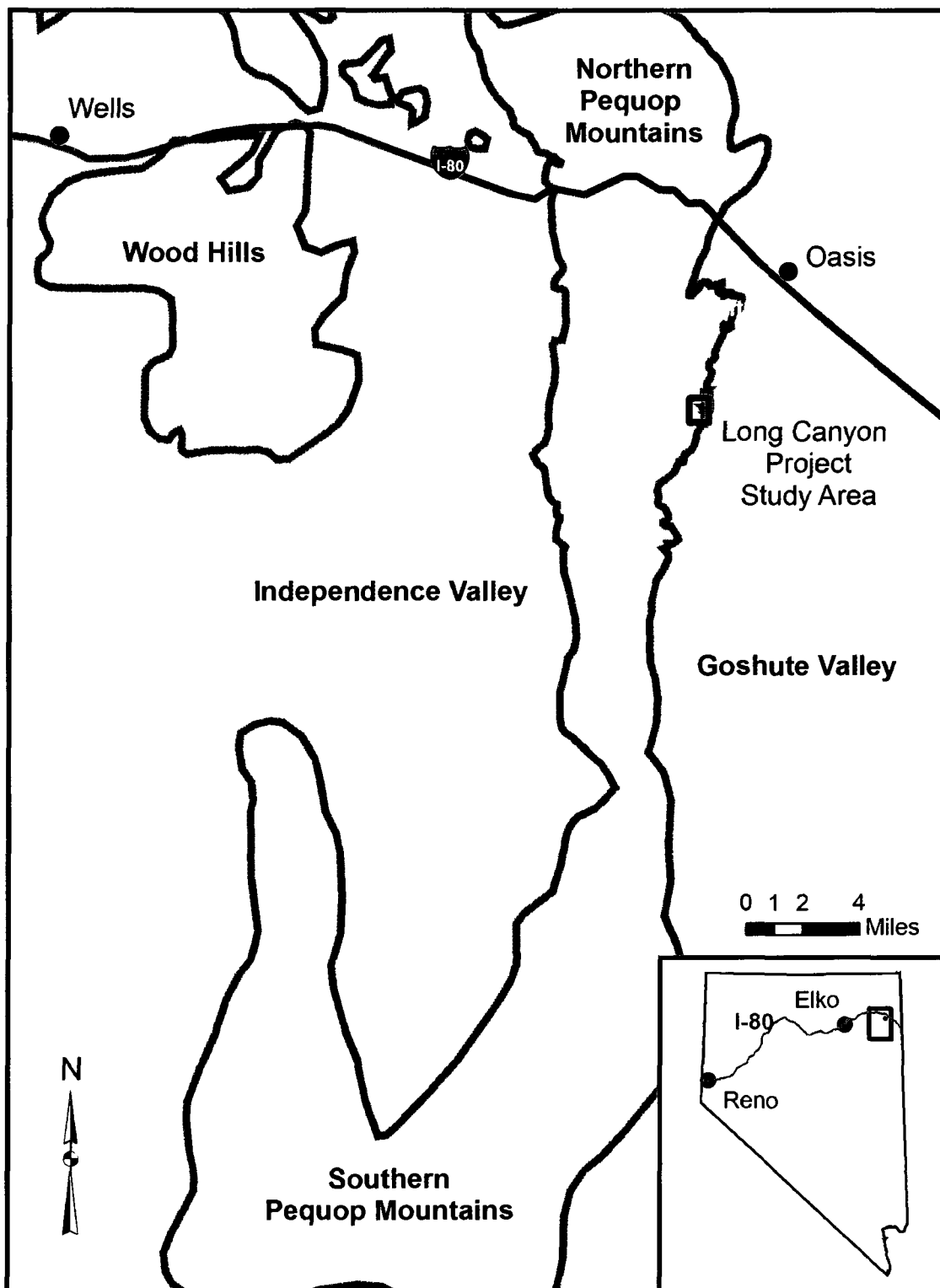


Figure 1. Location map of Long Canyon prospect. Based on maps by Thorman (1962) and Camilleri (1994).

Previous Work

Early geologic and structural mapping of the Northern Pequop mountains was carried out by C. H. Thorman (1962). He mapped the Pequop Mountains and separated them into several distinct structural units. In the structural area that encompasses the study of this thesis, Thorman made note of fine-grained limestone that weathered reddish brown and had light gray cherty lenses as well as a nodular, argillaceous, fine grained, medium gray limestone with small chert lenses that weathered reddish tan to pale orange-gray. The observations of weathering colors probably reflect the Fe-oxide minerals and alteration now observed within the study area. Later geologic and structural mapping was performed by Camilleri (1994) who identified [in the study area] both upper Cambrian Notch Peak limestone and dolostone, in addition to the Ordovician Pogonip Group Limestones. Prior to this, Thorman classified all carbonate rocks found within the study area as belonging to the Pogonip Group. Though Thorman (1962) identified dolostones within Pogonip Group rocks found elsewhere within the Pequop Mountains, no mention of dolostones in the Long Canyon study area was made. The current geologic understanding of the project area, as discussed below, has been advanced by the ongoing exploration effort at Long Canyon.

Stratigraphy

The Pequop Mountains are composed primarily of Proterozoic to Triassic miogeoclinal units of metamorphosed and unmetamorphosed carbonate and siliciclastic strata, and Tertiary volcanic and clastic units (Camilleri, 1997). The Cambrian to Ordovician age units present within the study area are discussed below. Unit names and numbered

abbreviations are based on the classifications provided by the staff of Frontier Development USA Inc. according to Smith (2009a). A stratigraphic column of the units discussed below is presented as *Figure. 2*.

Notch Peak Formation

The oldest exposed unit within the study area as well as the primary host rock for samples in this study is the Upper Cambrian Notch Peak Formation. The Notch Peak Formation was first described in the House Range of western Utah by Walcott (1908 a & b). The House Range exposure was formally subdivided into three members by Hintze *et al.* (1988) with refinements made by Miller *et al.* (2001). A regionally extensive unit, widespread in the central Great Basin, the Notch Peak Formation caps all Cambrian sequences in the Wendover region of the Utah-Navada border (McCollum and Miller, 1991). The first recognition of the Notch Peak Formation in the Pequop Mountains was made by Camilleri (1994), who also mapped it as the uppermost Cambrian unit exposed in the Wood Hills to the west of the Pequop Range.

Enp1

A massive dolostone unit, 20-30 m thick was mapped by Frontier staff at the southernmost extremity of Long Canyon Ridge. A unit tentatively classified as belonging to the Candland Shale (€cs) is locally exposed underlying Enp1 (Smith, 2009a) (Fig. 2).

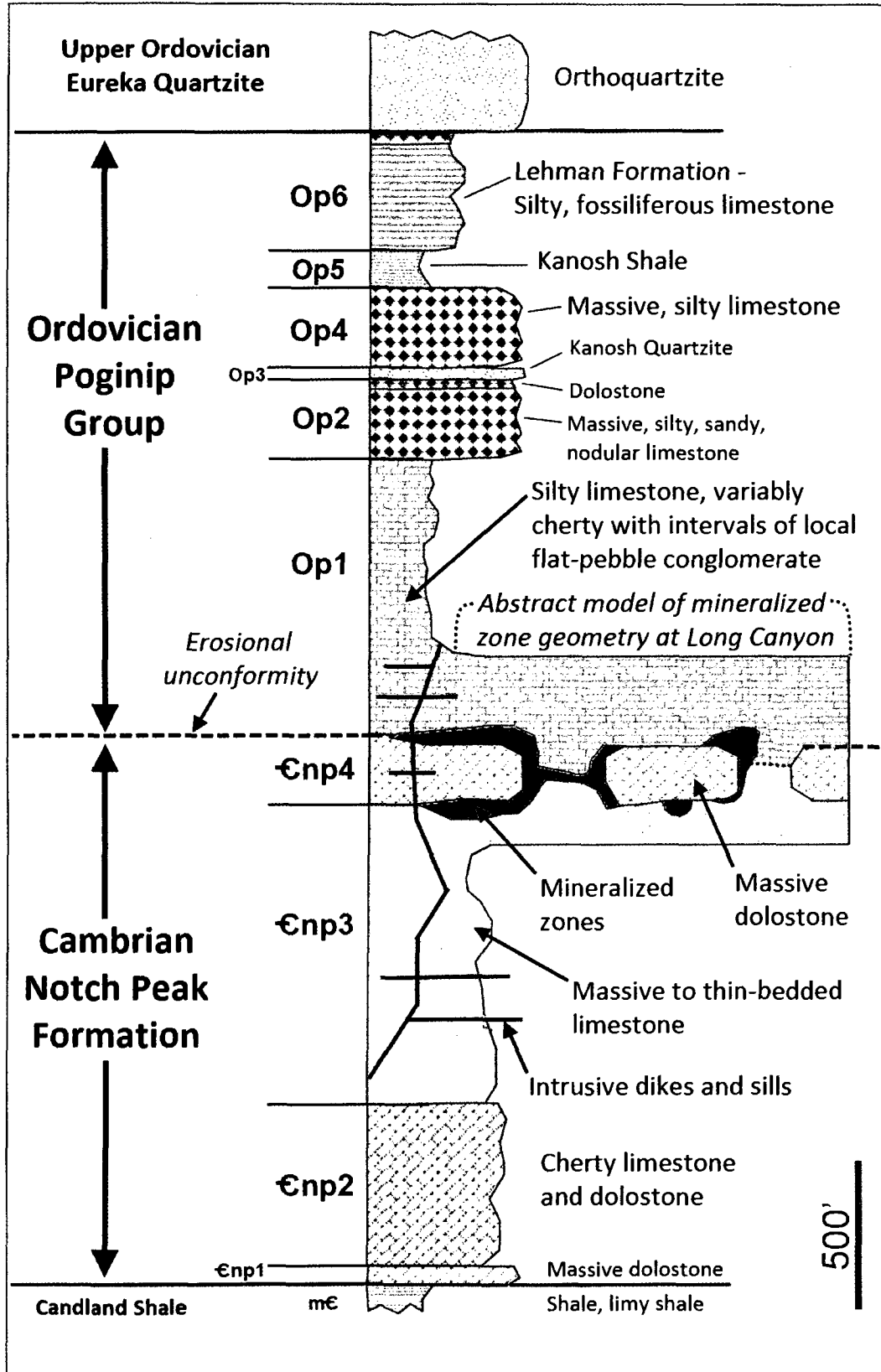


Figure 2. Stratigraphic column of Long Canyon (modified from Smith, 2009a.)

€np2

Above €np1 is a unit of unknown thickness of massive dolostone and limestone inter-layered with chert ribbons 3-5cm thick (Smith, 2009a).

€np3; Notch Peak Limestone

The lowest unit of the Notch Peak Formation sampled in this study is a recrystallized, bioclastic, massive to thin-bedded limestone, at least 190 m thick, that Thorson (2007) describes as being deposited in a predominately shallow marine or lagoonal environment in a series of at least four shallowing-upward cycles. This unit is the primary host for mineralized samples collected for this study. This unit contains local dolostone lenses.

€np 4; Notch Peak Dolostone

The capping unit of the Notch Peak Formation is a dolostone consisting of massive slabs, up to 70 m thick (Smith, 2009a), of dark to light gray, coarse crystalline dolostone that partially overlie the Notch Peak Limestone. Locally the Notch Peak dolostone slabs contain zebra texture, alternating layers of light colored, coarsely crystalline and dark colored, typically finely crystalline dolostone. Thorson (2007) reported that the dolostone unit appeared to be an additional third order shallowing cycle of dominantly coarse bioclastic debris. Thorson (2007) further proposed that these sediments were overlain by a lagoonal or sabka environment. The evaporation of seawater in such an environment resulted in a magnesium enriched fluid responsible for early diagenetic dolomitization of the underlying carbonate. Local zebra-textured dolostone is believed to

be the result of dissolution of bedding parallel evaporite nodules that were later infilled by dolomite after the primary dolomitization of the protolith (Thorson, 2007). The Notch Peak dolostone was likely exposed for several million years during a global sea level low stand at the end of the Cambrian resulting in an erosional unconformity between it and the overlying Pogonip Group of limestones. Karsting of the uppermost Notch Peak Formation dolostone unit likely formed at this time (*Fig. 2*). It is believed that karsting within the dolostone may be partially responsible for the eventual shape of the individual dolostone blocks produced during the boudinage event discussed in the following section on structure (Smith, 2009a).

Ordovician Pogonip Group

Nolan (1956) wrote on the history and usage of the term “Pogonip” as a stratigraphic group, which has changed in meaning over time. Its modern usage restricts the use of the term Pogonip to those sedimentary units between the Cambrian-Ordovician boundary and the Middle Ordovician Eureka Quartzite. The entire Pogonip Group is suspected to be as much as 600 m thick in the area of Long Canyon. (Smith, 2009a).

Op 1; Pogonip Limestone

Overlying the Notch Peak Formation is a unit of Ordovician [aged] Pogonip Group limestone (*Fig. 2*). Camilleri (1994) describes the Pogonip limestone as consisting of a gray, silty laminated limestone above a basal cherty limestone. This basal unit of the Pogonip Group is classified by Fronteer staff as belonging to the Park City Formation (Op1, *Fig. 2*) (Smith, 2009a). Several samples in this study, both mineralized and

unmineralized, were taken from this unit in addition to those taken from the Notch Peak Formation. As exploration and drilling has progressed on the site, this unit of Pogonip Group limestone has been found to be a better host for gold than those portions of the Notch Peak limestone that have been explored to date. This is believed to be, in part, a function of the more silty nature of Pogonip sediments as opposed to Notch Peak sediments (Smith, 2009b).

Overlying Pogonip units

The following units were not sampled as part of this study and are discussed only in limited detail based on their current understanding by project geologists on the site.

Overlying Op1 is Op2, the Big Springs Member (*Fig. 2*), a newly subdivided section of the Park City Formation. It is described as a massive, cliff forming unit of heavily burrowed limestone. Unit Op3 is a white cross-bedded quartzarenite reported to be approximately 15 m thick. It is interpreted to be the local exposure of the Kanosh Quartzite that Thorman (1970) described in the Wood Hills. Op4, the Oasis Limestone, is reported to be a fairly massive silty limestone with burrows similar to Op2. Op5 is a rarely exposed zone of shale known regionally as the Kanosh Shale. The shale is most commonly observed as a zone of olive or gray shale with thin bedded silty limestone weathered out on the surface. Op6, the Lehman Formation, is a massive gray limestone characterized by abundant buff to red silty “wisps”. Overlying the Pogonip Formation, to the north of the study area, are the Ordovician Eureka Quartzite, the Silurian Fish Haven Dolomite and the Permian Pequop Formation (Smith, 2009a).

Structure

The structural history of the Pequop Mountains is not yet fully understood. In the time since the initiation of this study the geological staff of Frontier Development USA Inc. have developed a structural model at Long Canyon to explain the unique geometry of Carlin-type gold deposits at the prospect. A full and detailed examination of the complex structural history of the Pequop Mountains or the Long Canyon prospect is beyond the scope of this work. What follows is a brief summary of the current structural model as it applies to gold deposits in the Notch Peak and Pogonip carbonate units in the Pequop Range. Previous structural models for the Pequop Mountains can be found in the works of Thorman (1962 & 1970) and Camarelli (1994 & 1997).

The most important structural features at Long Canyon in relation to known ore zones are boudinaged blocks of Notch Peak Dolomite. It is believed that during the Jurassic Elko orogeny, defined by Thorman *et al.* (1992), the area of Long Canyon was subjected to an extensional event. As a result of this extension, the Notch Peak dolostone (Cnp4) underwent brittle deformation and broke into irregular shaped boudins, while the underlying and overlying limestone units deformed more ductily. As a direct result of the boudinage, the surrounding limestone was folded into the space between the separated dolostone blocks. The underlying Notch Peak limestone produced anticlinal folding while the overlying Pogonip limestone formed synclinal folds as well as collapse features. As a result the Notch Peak limestone (Cnp3) and Pogonip limestone (Op1) units are in direct contact with one another between the boudin blocks of the Notch Peak dolostone unit (Cnp4). Mapping of synclinal folding in the Pogonip limestone has proven

successful in predicting the geometry of dolostone boudins in areas where they are not exposed at the surface. Inter-boudinal folding in the limestone units is most intense at the dolostone block margins where beds can display a vertical or locally overturned orientation (Smith, 2009a).

A later more brittle “kink” folding event is believed to be overprinted on the limestone units after the inter-boudinal folding. This was followed by regional NE trending folding. Fault sets, believed to be Eocene, include low-angle normal faults, NE trending high-angle normal and NW trending high-angle faults. Post-Eocene faulting includes N to NE-trending basin and range faulting along with other N trending fault sets (Smith, 2009a). Structural preparation is a key factor in the focusing of mineralization at Long Canyon. Mineral zones at Long Canyon occur predominantly in limestones along dolostone boudin margins as well as along NE-trending structures closely associated with dolomite boudins (*Fig. 2*).

Methodologies and Data

Field Mapping

An alteration map of the study area is provided on *Plate 1*. The alteration depicted was mapped by the author in the month of July, 2008. Lithologic boundaries are based after maps provided by New West gold in 2007. The area south of 4538200m N was mapped by the author in July, 2007. Structural information was collected during both the 2007 and 2008 field seasons. All maps provided in this thesis were generated using Arc View GIS software. Two cross sections, A-A' and B-B', are provided on *Plate 2*. Cross sections were constructed using Autocad software and are based on their surrounding drill logs as well as the author's field observations.

Sampling

In total, 63 samples were selected for analysis. A detailed sample location map is presented on *Plate 3*. All but one sample were collected between May and August of 2007. Sample LC08ZJ001 was sampled in July, 2008. The numbers for these samples are not consecutive. The analyzed samples were selected from a total of more than 170 samples initially taken. They were selected as best representing the relevant lithologies and observed alteration styles at the time of their sampling. The remaining samples were described in hand specimen, but are not individually discussed or located on any maps presented here.

Samples were collected from three carbonate units: the Notch Peak limestone (Cnp3), the overlying Notch Peak dolostone (Cnp4), and the basal Pogonip Limestone (Op1) units. Most of these samples were taken from roadcut exposures over the mineralized intervals where the samples could be observed in relation to various structural features and specifically limestone/dolostone contacts. Locally samples were taken from outcrops exposed at the surface. Jasperoids were sampled at four locations. A total of eight intrusive samples were taken. Five of the intrusive samples are from float. In each case the float material was followed up slope to ensure sampling took place as close to the intrusive source as possible. Two samples of in-situ, mineralized intrusive were samples from a single intrusive dike swarm found in road cut exposures. A single sample of an unmineralized intrusive rock was also collected from drill roadcut exposures.

Thin Sections

Splits taken from samples taken during the 2007 field season were sent for the professional production of polished thin sections. Sample LC08ZJ001 was sectioned by the author. Individual petrographic descriptions accompanied by annotated photomicrographs for each sample are included in appendix A.1 in the CD appendix found in the back of this thesis. Appendix A.2 contains the images associated with each thin section description. Included are all photomicrographs, scanned thin section images, SEM images, EDS spectra, and X-ray diffraction patterns.

XRD

For preparation of XRD analysis, a split of each sample was crushed, to produce an acetone slurry that was applied to a standard thin section-sized glass slide. Tools were washed clean with acetone between each sample. For each sample the X-ray diffractometer was set at 40kv and 30MA. Each sample was analyzed over a range of at least 5-50 degrees, with individual steps of 0.02 degrees, with a dwell time of 0.6 seconds per step. X-rays were produced using the XRG 3100 X-ray generator maintained by the Nevada Bureau of Mines and Geology. Instrument control was performed using MDI Data Scan 4. Mineral interpretations were generated using MDI Jade 6.5. X-ray diffraction patterns with mineralogical interpretations are included in Appendix A.2. A summary table of the results of XRD analysis is presented at the end of Appendix A.1.

SEM

Selected samples were analyzed in the scanning electron microscope (SEM) laboratory at the University of Nevada, Reno. Samples were analyzed over three separate afternoon sessions during the months of November and December, 2008. Technical support and operation were provided by UNR associate professor Dr. John McCormack. SEM results, annotated SEM images and photomicrographs are included in the individual thin section descriptions located in Appendix A.1.

Geochemical Analysis

All samples were subject to chemical analysis including whole rock oxide analysis (by ALS Chemex), 30g Au Fire Assay, and 72 element ICP geochemistry (by American

Assay Laboratories). A table of the geochemical results of samples examined in this study is provided in Appendix B. Prior to working with the data, all values for whole rock oxide analysis were normalized such that all values obtained (including LOI) summed to a total of 100% for each sample. Additionally all statistical analysis and graphs of the geochemical data of samples analyzed in this report were produced after all “non-detect” values were set to a value equal to one-half the analytical detection limit.

Geochemical data were analyzed by comparing statistical correlations of the various chemical constituents to one another, most notably Au. For each constituent pair a Pearson product-moment correlation coefficient (r) was generated using Microsoft Excel.

$$r = \frac{n \sum xy - (\sum x)(\sum y)}{\sqrt{[n \sum x^2 - (\sum x)^2][n \sum y^2 - (\sum y)^2]}}$$

Where x and y = the data for the elements being compared and n = the number of ordered pairs of those elements in the data set.

Correlation coefficients (r) were tested to determine their statistical significance using the students t – distribution test

$$t = \frac{r}{\sqrt{\frac{1-r^2}{n-2}}}$$

where r = the coefficient of correlation and n = the number of ordered pairs of those elements in the data set. The resulting t value was compared to a target (t_c) to determine the probability that a given value for r was significantly different from a value of zero. Tables of correlation coefficients (r) and calculated t statistics for data from samples collected in this study are included in Appendix C.

Additionally for each data set chemical plots were generated of Au vs. each analyzed element (Appendix D.1).

In addition to the chemical analysis of samples collected for this study, data from exploration sampling were provided to aid in determining the chemical associations with gold at Long Canyon. Like the samples collected for this study, all “non-detect” values in the exploration data sets were set at a value of one half the detection limit. These data included geochemical results from rock and soil samples collected on site between January, 1999 and July, 2007 as well as chemical analysis of drill holes from 2006 and 2007 drilling programs. Only those rock and soil data from samples that were located in the immediate study area for this project were examined for statistical relationships between the analyzed chemical elements and gold. A map showing the distribution of those samples is provided on Plate 4.

All three exploration data sets were examined for the statistical correlation of the analysed elements to gold using the method described above. The results of these analyses are discussed but the statistical data sets that were generated are not provided in this study. Graphs of Au vs. selected chemical constituents analyzed for the soil, rock, and drill data sets are available in Appendices D.2, D.3, and D.4, respectively. Maps of soil anomalies for Au, As, Sb, and Hg were generated using ArcView GIS kriging tool. They can be found on Plates 5a, 5b, 5c, and 5d, respectively.

Carbonate Alteration and Mineralization

In addition to primary sulfidation and Au enrichment, the host rocks of Carlin-type deposits are typically decarbonated, argillized and variably silicified (Cline, 2005). Like other Carlin-type deposits, gold at Long Canyon is associated with decarbonation and variable degrees of silicification in carbonate host rocks. As previously noted, gold at Long Canyon is focused around boudin margins and other boudin related structures where deformation of the limestone host is greatest (Smith, 2009a). An alteration map of the study area with sample locations is provided on Plate 1. Cross sections are provided on Plate 2.

Decarbonatization

Decarbonatization is the primary alteration process associated with gold deposits at Long Canyon (Figs. 3 & 4). Decarbonatization is a result of dissolution of calcite and to a lesser extent dolostone units under acidic conditions. Additionally, dissolution of carbonate minerals created features such as dissolution-collapse breccias, and cave fill sediments. These features form favorable host rock for gold due to their increased permeability.

Loss of carbonate is reflected texturally as well as chemically in many of the highest grade samples. Sample LC07ZJ086 is a sanded portion of the Notch Peak Limestone and likely represents post-karsting cave fill sediments (Fig 5). This sample retains only 5% secondary calcite. Loss of carbonate has resulted in the concentration of quartz silt, Fe oxides, and trace muscovite/sericite.

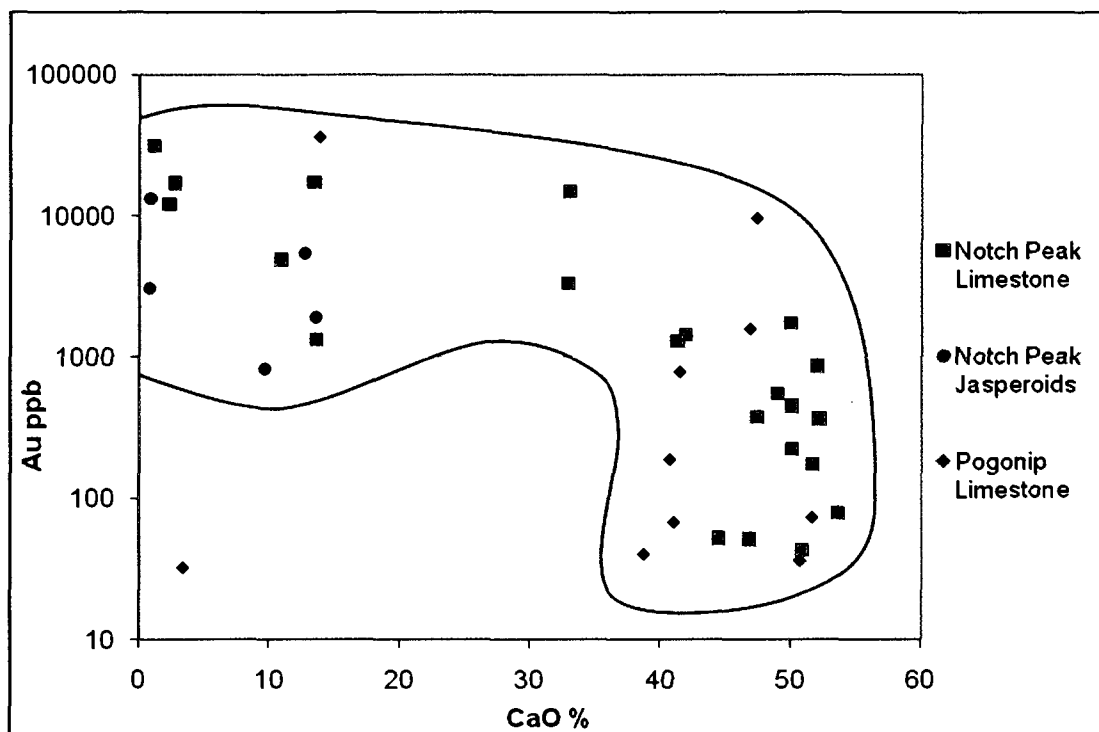


Figure 3. Decarbonatization effects on limestone host rocks vs. Au mineralization.

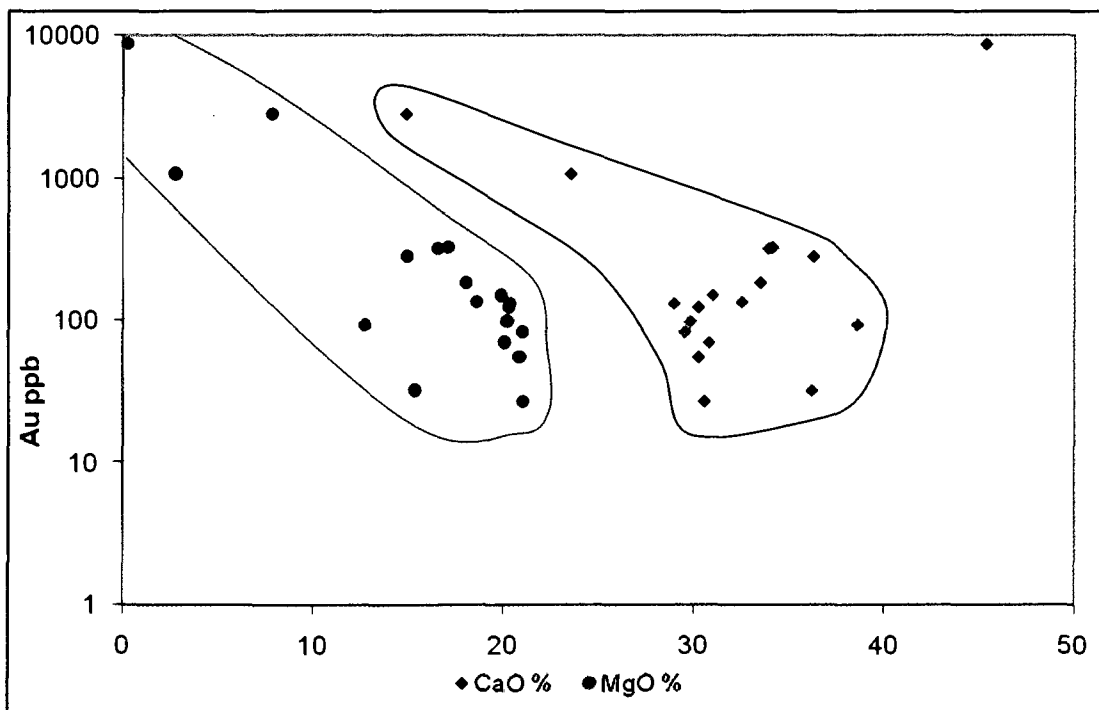


Figure 4. CaO and MgO values for samples Notch Peak dolomite vs. Au. The few samples of dolostone that are strongly mineralized are clearly decarbonatized.

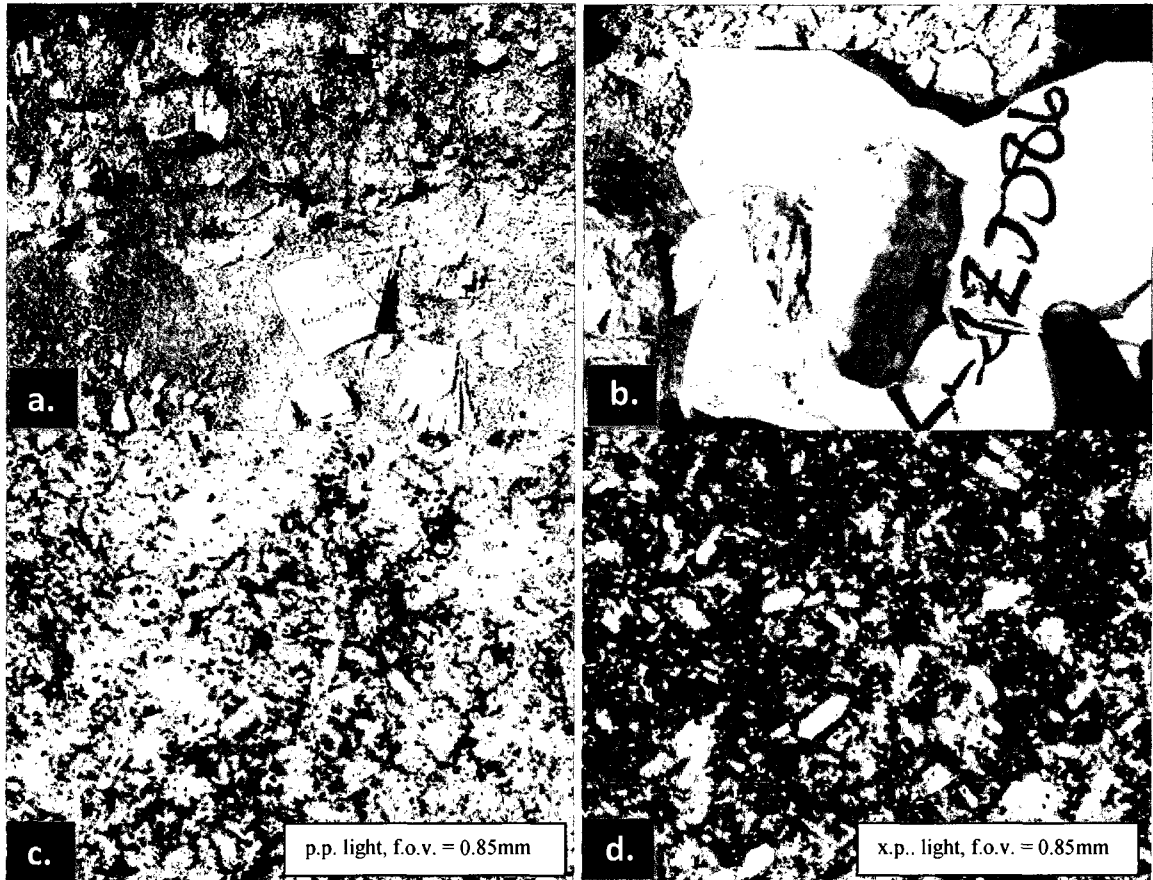


Figure 5. Sample LC07ZJ086. a.) road cut view, b.) hand sample, c.) and d.) are photomicrographs in plane polarized and cross polarized light of bipyramid quartz grains displaying incipient, reticulate silicification of the ore host.

Carbonate remobilization is common in both mineralized and un-mineralized carbonate host rock at Long Canyon. Reprecipitation of calcite as veins does take place after gold precipitation (Fig. 6) and likely takes place at earlier stages as well. In unmineralized rocks, 1-2mm calcite veins are locally present and commonly form along joints.

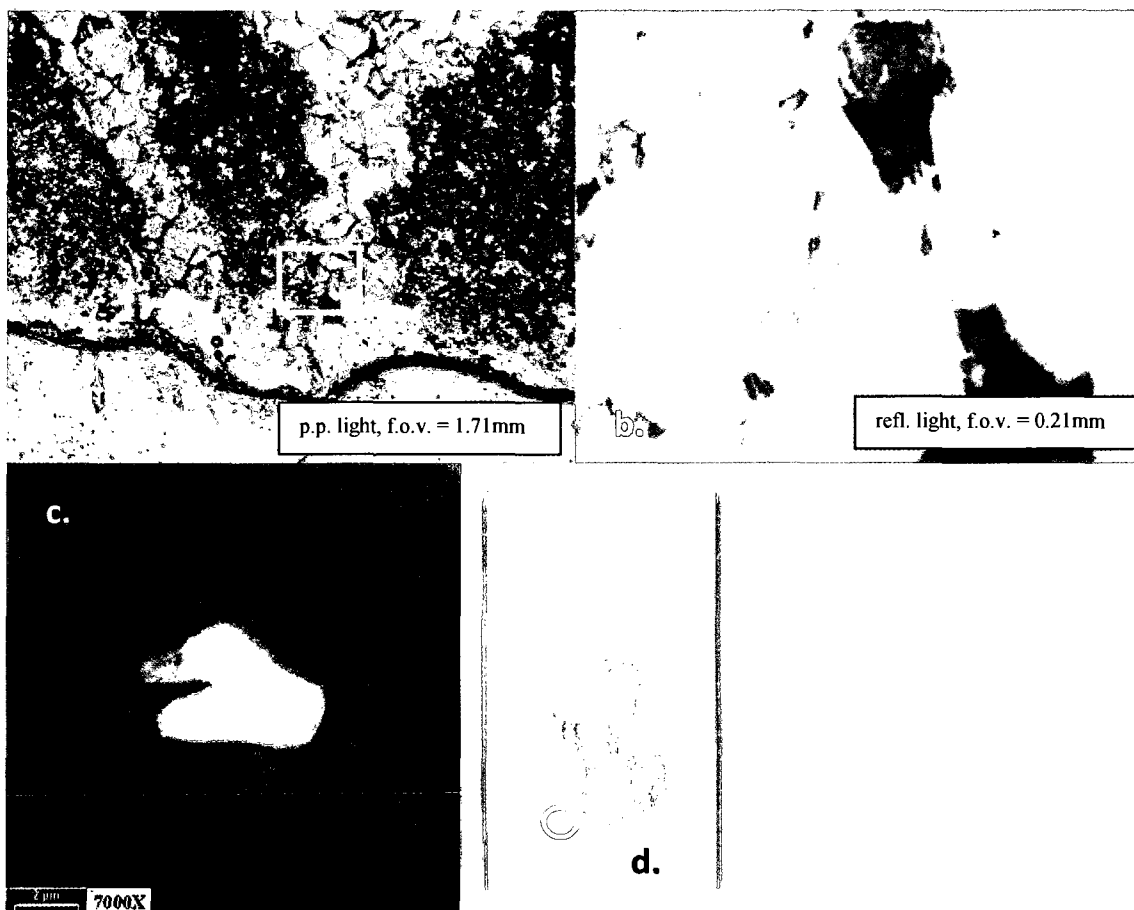


Figure 6. Sample LC07ZJ083. a.) late calcite vein in mineralized Notch Peak Limestone with box showing location of Figure 6 b., b.) gold grain in calcite vein, c.) SEM image of gold grain in Figure 6 b., d.) scan of thin section showing photo location and several calcite veins.

Silicification

Typical of Carlin-type mineralization, some silicification associated with gold mineralization is observable at Long Canyon(Fig. 5). Several small outcrops of jasperoid or silicified limestone are present at Long Canyon. Many of these outcrops are only partly silicified and still contain measurable calcite. On the whole, true jasperoids are considered to be volumetrically insignificant compared to decarbonated host types such as sanded carbonates, solution/collapse breccias, and cave fill sediments.

The importance of silica introduction in the mineralizing process becomes more apparent upon examination of sample chemistry and compilation of petrographic data. For example, the heavily decarbonated sample LC07ZJ086 shows no evidence of introduced silica when examined in hand sample. However, when viewed in thin section (Figure 5, c. and d.) it shows excellent examples of doubly terminated quartz crystals caused by incipient silicification over preexisting silt sized quartz grains. It is interpreted that the orientation of quartz grains present in sample LC07ZJ086 (Fig. 5, c. and d.) and other similarly sanded samples of decarbonated limestone, resemble the reticulate texture commonly observed in mineralized jasperoid samples examined in this study (Fig. 7).

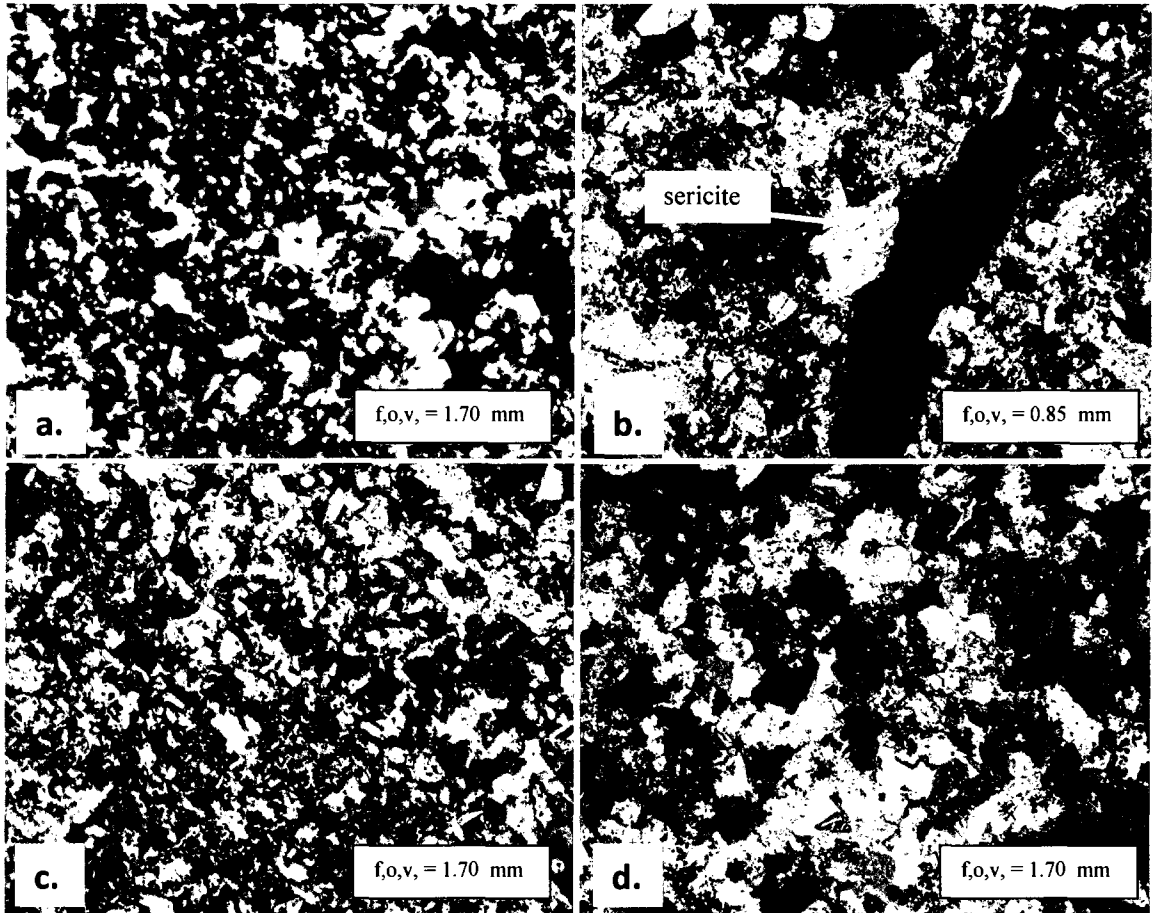


Figure 7. Jasperoid photomicrographs in cross polarized light; a. & b. LC07ZJ066, b. sericite along fracture., c. particularly good example of reticulate texture in sample LC07ZJ170, d. local remnant calcite in sample LC07ZJ081A.

Table 1 shows selected whole rock oxide results for samples of Notch Peak limestone and jasperoids. A clear increase in percent SiO_2 and a clear decrease in percent CaO accompanies an increase in gold. Figure 8 illustrates the increase in gold associated with an increase in silica content.

SAMPLES	Au_ppb	SiO ₂ %	CaO %	MgO %	Fe ₂ O ₃ %	TiO ₂ %	Lithology
LC07ZJ 156	31010	86.92	1.18	0.49	2.02	0.24	Cnpls
LC07ZJ 126	16940	54.38	13.44	1.62	2.64	0.44	Cnpls
LC07ZJ 153	16810	83.18	2.74	0.55	2.14	0.26	Cnpls
LC07ZJ 125	14700	23.87	33.03	1.51	1.93	0.33	Cnpls
LC07ZJ 170	13300	93.56	0.78	0.23	0.19	0.31	Jasperoid
LC07ZJ 152	11920	88.26	2.31	0.57	0.11	0.2	Cnpls
LC07ZJ 81 B	5427	71.34	12.71	0.3	0.67	0.16	Jasperoid
LC07ZJ 086	4803	72.1	10.91	0.62	1.06	0.18	Cnpls
LC07ZJ 155	3264	31.47	32.9	0.65	0.88	0.31	Cnpls
LC07ZJ 077	3094	94.05	0.76	0.18	0.74	0.09	Jasperoid
LC07ZJ 066	1919	59.18	13.5	7.38	0.36	0.03	Jasperoid
LC07ZJ 124	1721	7.63	49.95	0.67	0.27	0.02	Cnpls
LC07ZJ 083	1426	20.66	41.86	0.49	0.56	0.12	Cnpls
LC07ZJ 131	1301	62.06	13.59	1.88	1.47	0.27	Cnpls
LC07ZJ 092	1278	19.26	41.23	1.05	1.24	0.16	Cnpls
LC07ZJ 005	854	4.39	52.04	0.47	0.25	0.04	Cnpls
LC07ZJ 81 A	834	78.6	9.64	0.32	0.55	0.12	Jasperoid
LC07ZJ 088	542	7.57	49	1.32	0.33	0.06	Cnpls
LC07ZJ 157	447	6.41	50.06	0.39	0.34	0.1	Cnpls
LC07ZJ 091	374	9.06	47.42	0.78	0.88	0.14	Cnpls
LC07ZJ 158	364	4.32	52.2	0.3	0.27	0.06	Cnpls
LC07ZJ 067	282	2.95	36.32	14.97	0.12	< 0.01	Cnpd
LC07ZJ 130	223	2.89	50.08	3.12	0.25	0.02	Cnpls
LC07ZJ 056	174	3.53	51.63	0.49	0.14	0.02	Cnpls
LC07ZJ 048	151	2.7	31	19.93	0.36	0.04	Cnpd
LC07ZJ 094	135	1.72	32.54	18.62	0.17	< 0.01	Cnpd
LC07ZJ 050	93	2.45	38.61	12.75	0.22	0.03	Cnpd
LC07ZJ 149	78	1.69	53.59	0.71	0.13	0.04	Cnpls
LC07ZJ 168	52	12.94	44.45	1.04	1	0.13	Cnpls
LC07ZJ 169	51	9.13	46.81	0.97	0.57	0.09	Cnpls
LC07ZJ 016	43	5.96	50.87	0.41	0.29	0.05	Cnpls

Table 1. Selected chemical data for samples of Notch Peak limestone sorted by decreasing assay values. Notice that those rocks sampled in the field as “Jasperoids” do not necessarily have the highest silica values. Several are only partially silicified, evident by >10% CaO.

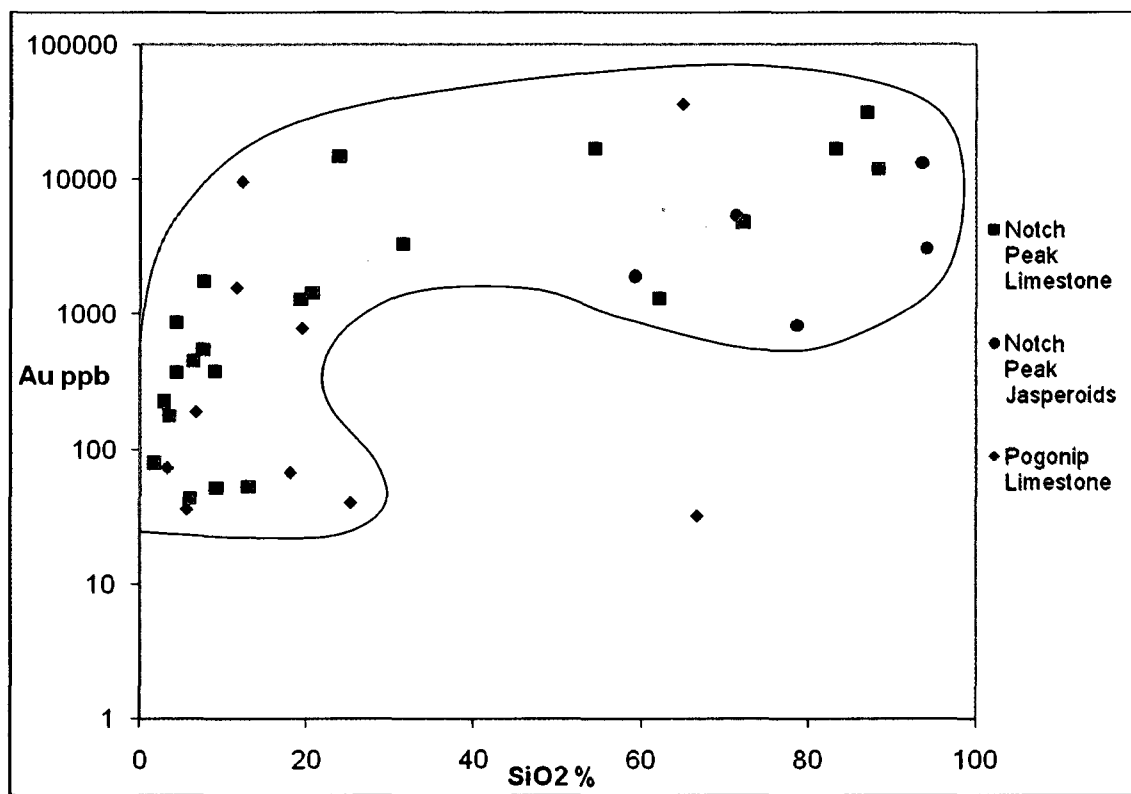


Figure 8. Silicification effects on limestone host rocks vs. Au.

Gold and Sites of Gold

Microscopic gold is [commonly] visible in several of the highest grade samples collected for this study. Gold occurs as blebs of native metal generally ranging from 2 to 5 μm in size. In total 5 samples from the Notch Peak Limestone, 2 samples from the Pogonip Limestone, and 1 jasperoid were observed to have optically identifiable gold in polished section. The gold at Long Canyon is relatively pure, having no substantial silver content. This is observed both in the geochemistry as well as SEM analysis of gold grains in this study. Figures 9 through 14 are images of native gold observed in this sample set.

Most examples of native gold observed in the sample set are like those pictured in Figures 9 through 12. They are not encapsulated in any single mineral grain. Locally gold can be observed encapsulated in calcite as is shown in Figure 6. Notably gold has been observed on the rim of a hematite pseudomorph after pyrite in sample LC07ZJ156, (Figs. 13 and 14). This is evidence of classic Carlin style gold mineralization in which gold is precipitated within arsenian pyrite forming as rims on preexisting pyrites.

Additionally a single example of gold encapsulated in quartz was observed in sample LC07ZJ054 (pictured in Appendix A.1). This is not unexpected given the strong evidence for silicification discussed above. While this was the only example of Au encapsulated in quartz observed, it does demonstrate that silicification was ongoing after the gold event(s).

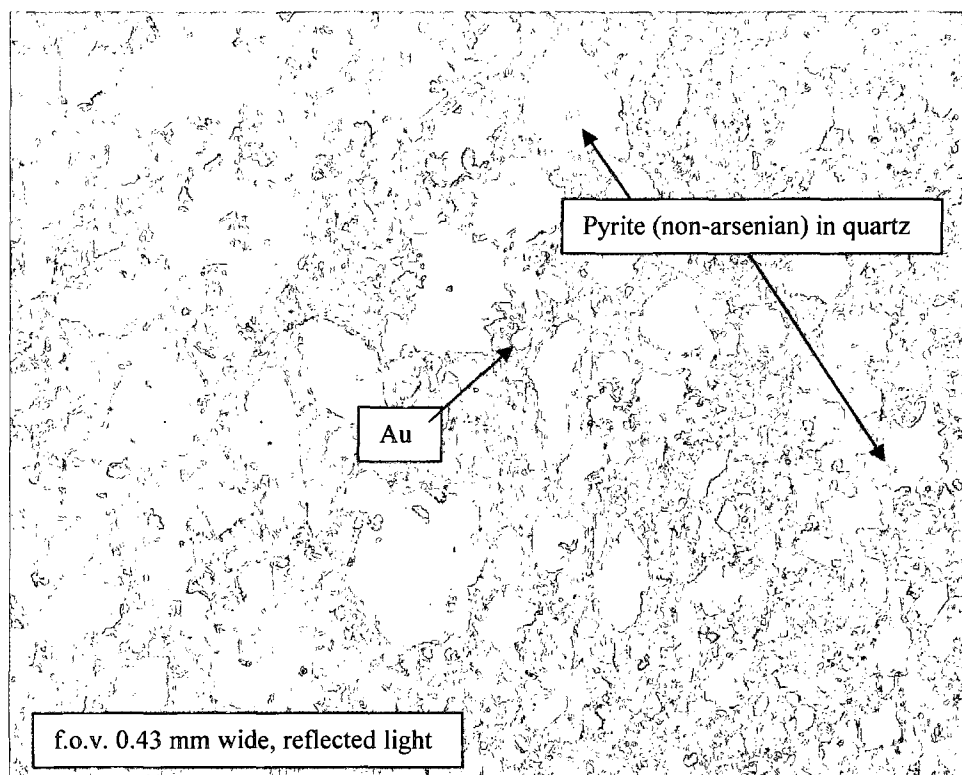


Figure 9. LC07ZJ153 Gold bleb in the center of the slide;
Notice several encapsulated non-arsenian pyrites in quartz grains; matrix is largely fine grained quartz with disseminated hematite and possible clays.

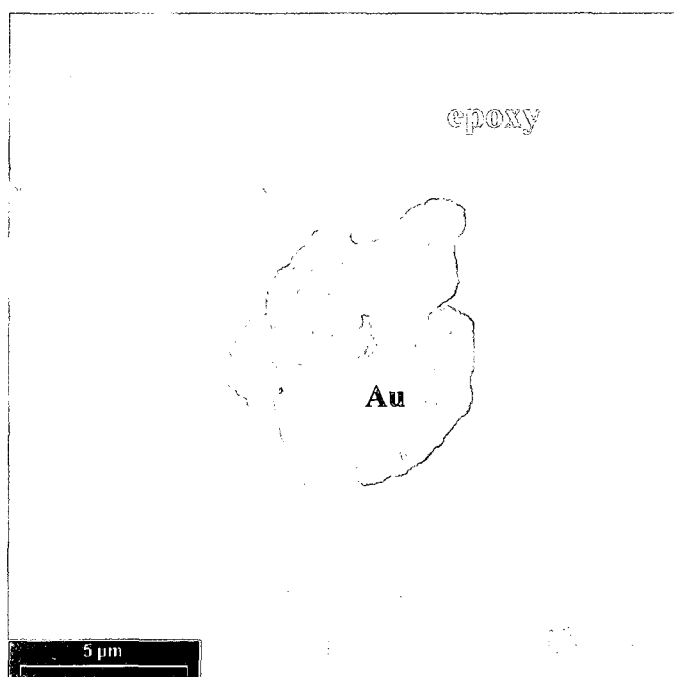


Figure 10. LC07ZJ153 SEM image of gold bleb pictured above.

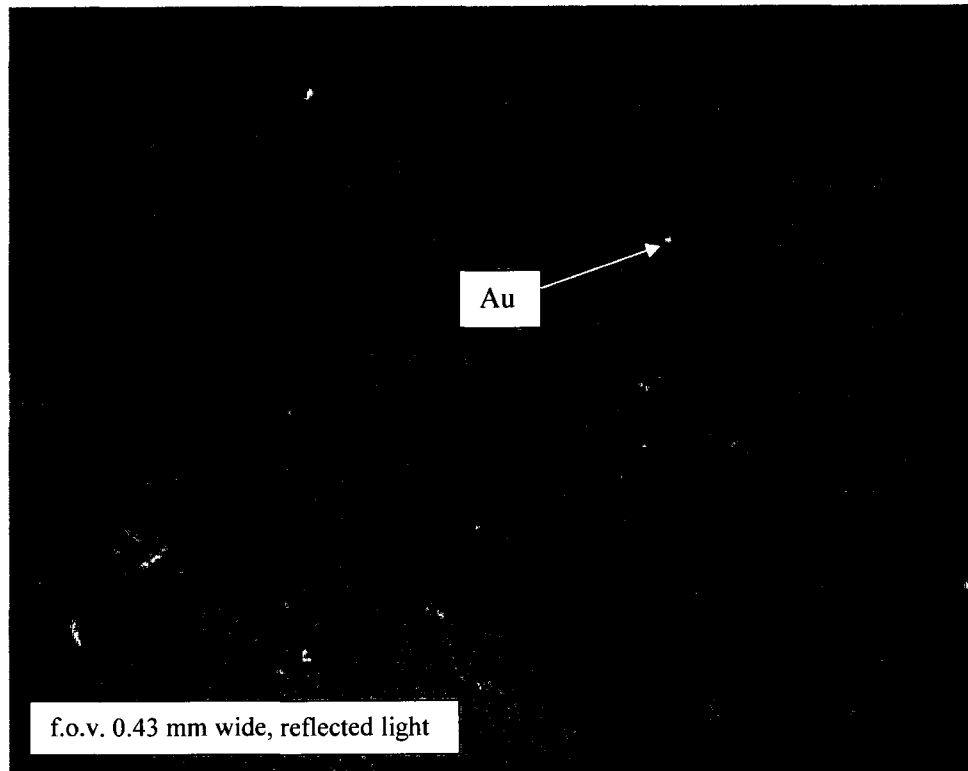


Figure 11. LC07ZJ126 gold bleb in decarbonated limestone.

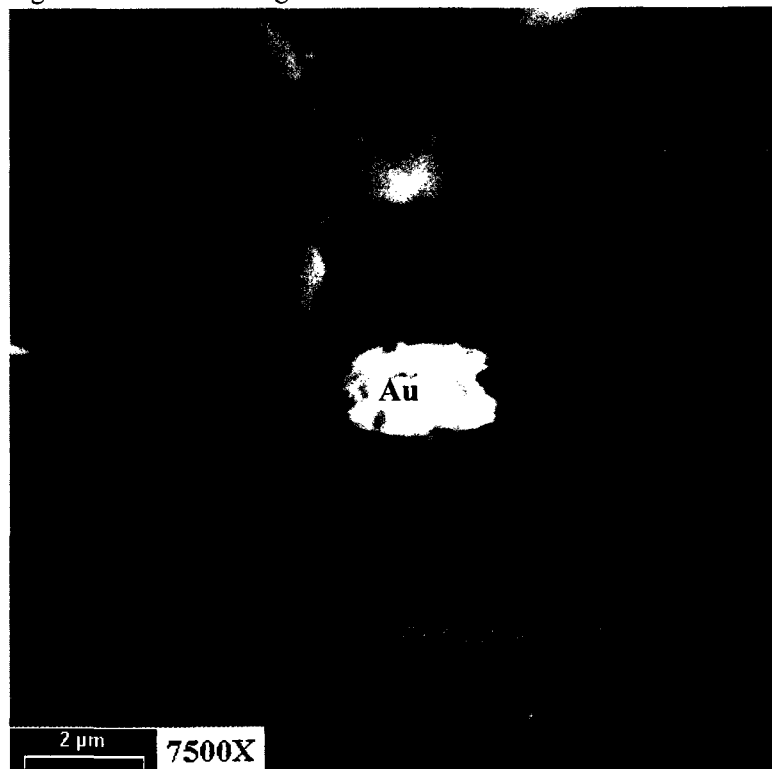


Figure 12. LC07ZJ126 SEM image of gold bleb pictured above.

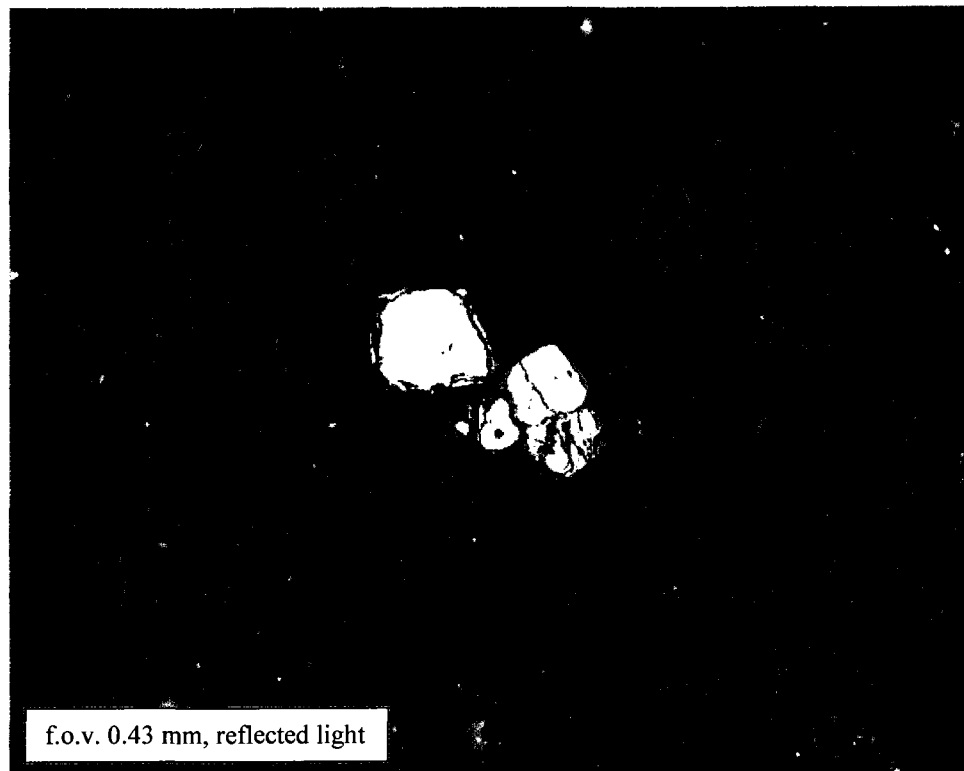


Figure 13. LC07ZJ156 Gold bleb on rim of hematite pseudomorph after pyrite. The matrix is Fe stained quartz grains. The sample looks similar to a jasperoid in plane transmitted light.



Figure 14. LC07ZJ156 SEM image of 2 gold blebs on rim of hematite pseudomorph after pyrite.

Fe Sulfides

Early diagenetic pyrite is common in all carbonate rock at Long Canyon. No marcasite or pyrrhotite was observed in samples examined in this study. Most commonly the pyrite has been completely oxidized to hematite and goethite pseudomorphs. However by far the majority of samples examined in this study have trace amounts of remnant, nonarsenian pyrite. This remnant pyrite is present in both strongly mineralized as well relatively unaltered carbonate rocks. In such cases, the preservation of sulfide under highly oxidizing conditions is a result of encapsulation by quartz (Figs. 15 and 16). Additionally, pyrite can also be preserved where encapsulated within single calcite grains, particularly in unmineralized samples. Remnant pyrite can be euhedral, but is most commonly anhedral. Typical sizes of preserved pyrite are on the order of <0.01 to 0.5 mm.

Locally, arsenian pyrite has been observed as rims on pyrite encapsulated in quartz. Surviving rimmed pyrites are very rare due to the intensely oxidized nature of the system. As such only three samples have been definitively recognized to contain arsenian rims on pyrites (LC07ZJ069, LC07ZJ083, and LC07ZJ153). Figure 17 is of the rimmed pyrite from sample LC07ZJ069. EDS spectra confirm that the rim on the pyrite is clearly arsenian. The spectra also appears to have a very small peak in the location at which gold would be expected to register on the spectra pattern (Fig. 17). The core of the rimmed pyrite is barren non-arsenian pyrite.

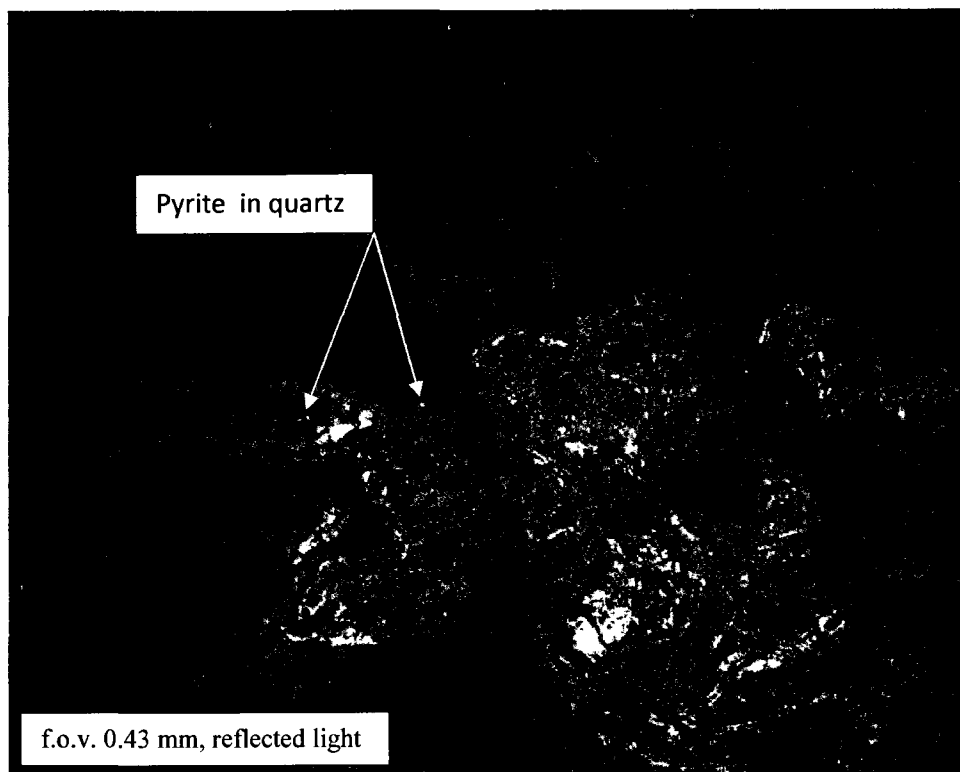


Figure 15. LC07ZJ126 Pyrite (not arsenian) encapsulated in quartz next to poorly polished hematite.

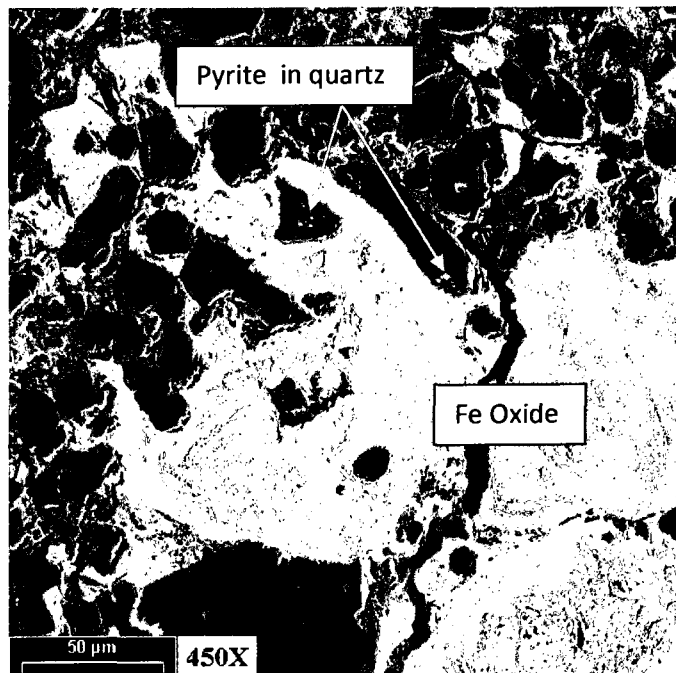


Figure 16. LC07ZJ126 SEM image pyrite in figure 15. EDS spectra confirm pyrite ID.

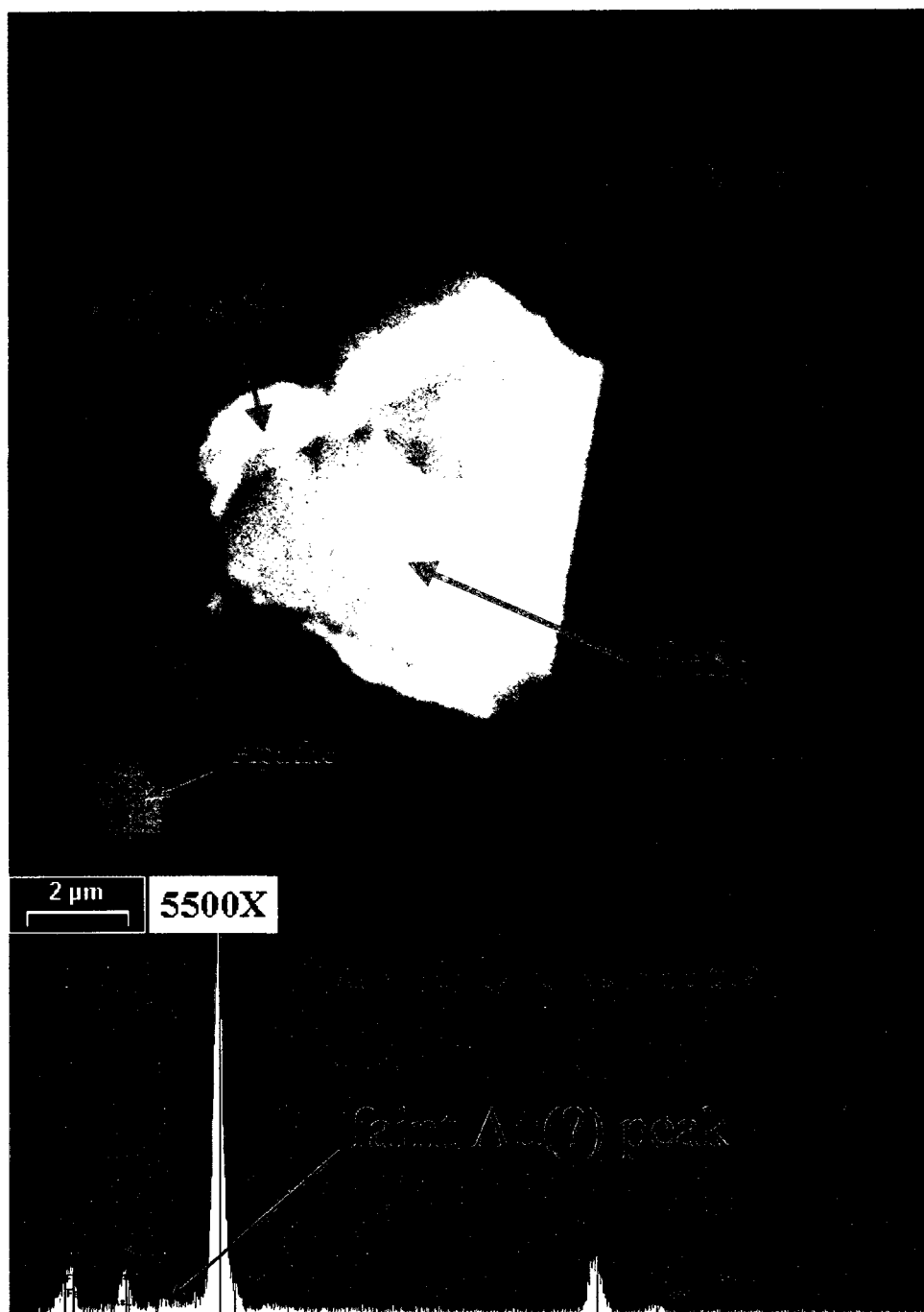


Figure 17. SEM photo and EDS spectra of arsenian rim on pyrite, encapsulated in quartz found in sample LC07ZJ069.

Additional Sulfide Minerals

In addition to the abundant pyrite and local arsenian pyrite observed in this sample set, traces of mercury sulfide (cinnabar) and arsenic sulfide (orpiment/realgar) were observed during SEM analysis of sample LC07ZJ153.

Fe Oxide

As stated previously, gold-bearing intervals at Long Canyon are intensely oxidized. Mineralized zones are strongly hematitic. In addition to hematite alteration, limonitic/goethitic zones of Fe oxides are common throughout the site. Frontier geologists have observed limonitic/goethitic zones to form halos around the more strongly oxidized hematite-rich ore zones. Jarosite and scorodite have also been locally described in mineralized rocks in the field (Smith, 2009a). The relationships of different oxides to one another can best be seen by looking at thin sections with the unaided eye. Figure 18 shows several scanned thin sections that show textural relations of the different oxide materials to one another. Sample LC07ZJ153 (Fig. 18a) appears to have been an earlier limonitic/goethitic material that was broken by later brecciation/deformation and was replaced by hematite. SEM backscatter results for both the light and dark red materials were nearly identical. Each had peaks for Fe, Si, O, and, Al, plus a weak peak for Mg. Mg indicated that fine illite in addition to Fe oxides may be present. In sample LC07ZJ126 (Fig. 18b), jarosite as well as illite is indicated in the XRD pattern. Figure 19 shows hematitic pseudomorphs after pyrite with lighter jarosite. Sample LC0ZJ125 (Fig. 18c) shows banded jarosite and hematite cut by a late calcite vein. This sample contains native gold in the matrix of hematite/jarosite and fine quartz with possible trace

kaolinite. Samples LC07ZJ86 and LC07ZJ091 also show hematite and jarosite but are not as strongly altered. Sample LC07ZJ086 appears to show hematite rimming earlier jarosite (Fig. 18d). Sample LC07ZJ101 shows disseminated limonitic/goethitic oxide in low grade Notch Peak dolomite.

Scorodite is less well represented in this sample set. A light green tint to some of the hand sample materials taken for samples LC07ZJ125 and LC07ZJ126 indicate that scorodite may be present. Scorodite was not observed by the author in thin section, nor was it recognized in XRD. Figure 20 is of local strongly scoroditic alteration along joints observed in road cuts during alteration mapping in July 2008.

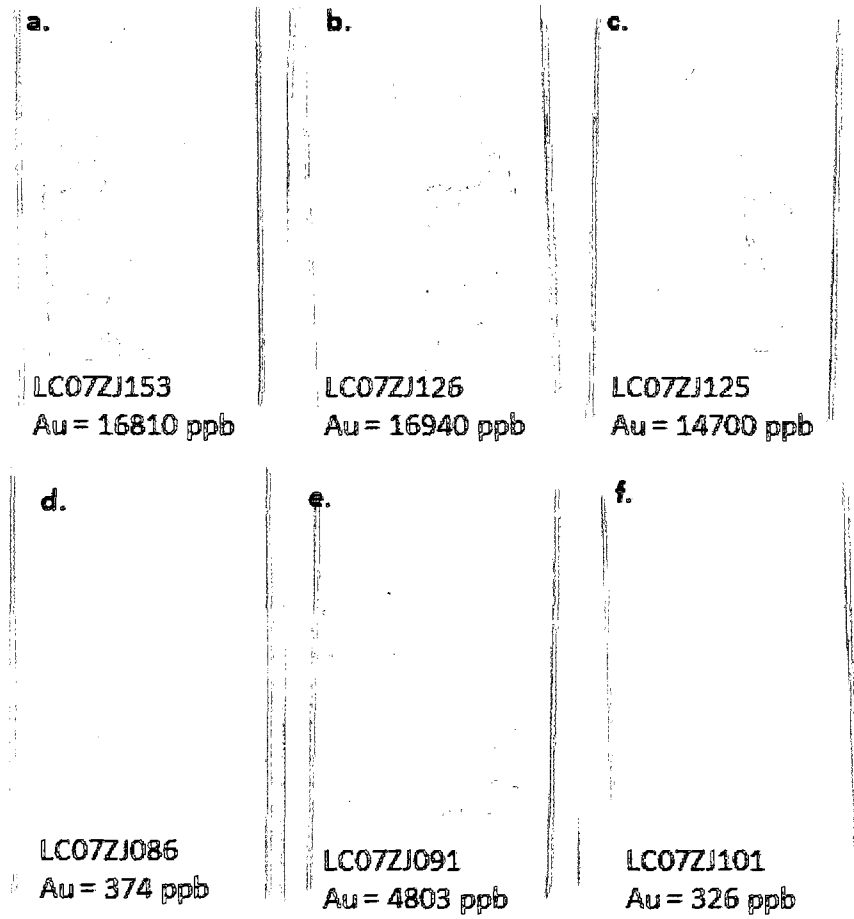


Figure 18. Pictures of oxide relations as viewed macroscopically in thin section.

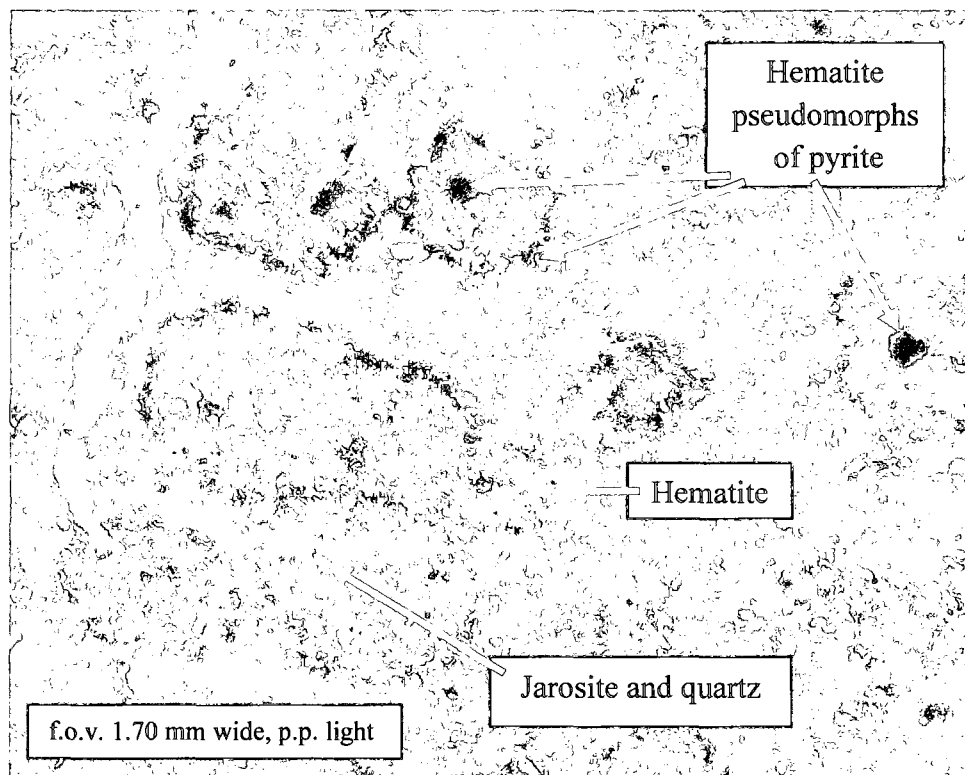


Figure 19. LC07ZJ126 Jarosite with hematite. The image is taken with the condenser lens engaged. The author believes that this exaggeration of the “true” colors better illustrates oxide differences in the sample.

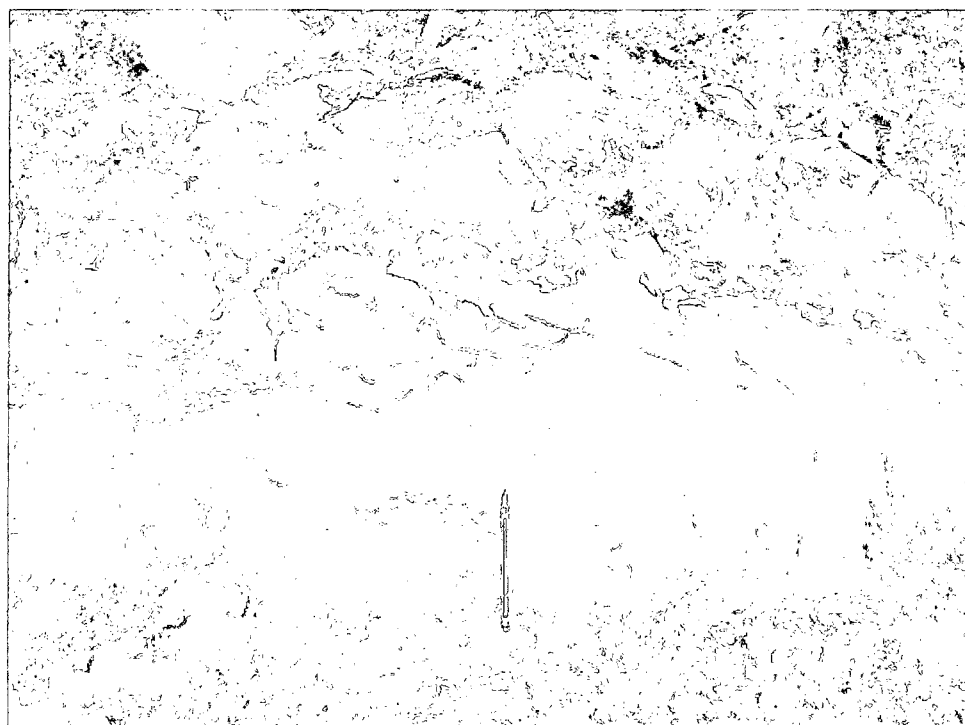


Figure 20. Joints that focus local (green) scoroditic alteration with hematite halos.

Illite and Sericite/Muscovite

Illite is indicated in the XRD patterns of Notch Peak samples LC07ZJ133 and LC07ZJ126, where it is likely a fine component of the oxidized matrix. Additionally, illite is optically indicated in sample LC07ZJ131. Generally speaking, illite and sericite (or very fine muscovite) are optically indistinguishable and as such determination via XRD is necessary to distinguish the two. Given the close proximity of sample LC07ZJ131 to that of LC07ZJ133, an illite identification for both is appropriate. Jasperoid samples LC07ZJ077 and LC07ZJ081A each have fine sericite/illite; however, it is in too little a concentration for either to be detected by the XRD. Illite is seen replacing biotite in the mineralized intrusive rocks discussed in the following section on intrusions.

Muscovite was detected in XRD patterns of 14 samples in this sample set. Optically it was only visible in trace amounts. It has been suggested by Frontier geologists that trace muscovite in the samples from Long Canyon is of an early metamorphic origin (Smith, 2009b). Muscovite observed in this sample set is not sedimentary in appearance and is likely due to alteration. Evidence that at least some of the muscovite is not depositional can be observed in sample LC07ZJ093 (slide b). Muscovite can be seen forming, post brecciation, in the breccia matrix (see photomicrographs in appendix A.1).

Carbonate samples examined in this study, in particular samples of limestone from the Notch Peak Formation, appear to show some visual correlation between Au and K

(Figure 21). Primary sericitic or potassic alteration however is not considered typical of Carlin-type deposits. Any correlation that may be present more likely results from illite and muscovite/sericite alteration favoring similar structural features as the gold deposition at Long Canyon. As shown in the following section on geochemistry, the samples examined for this study from the Notch Peak limestone show a statistical relation between Au and K. Other lithologic groups examined in this study do not. The geochemical analysis of drill holes at Long Canyon do show a weak statistical correlation between Au and K.

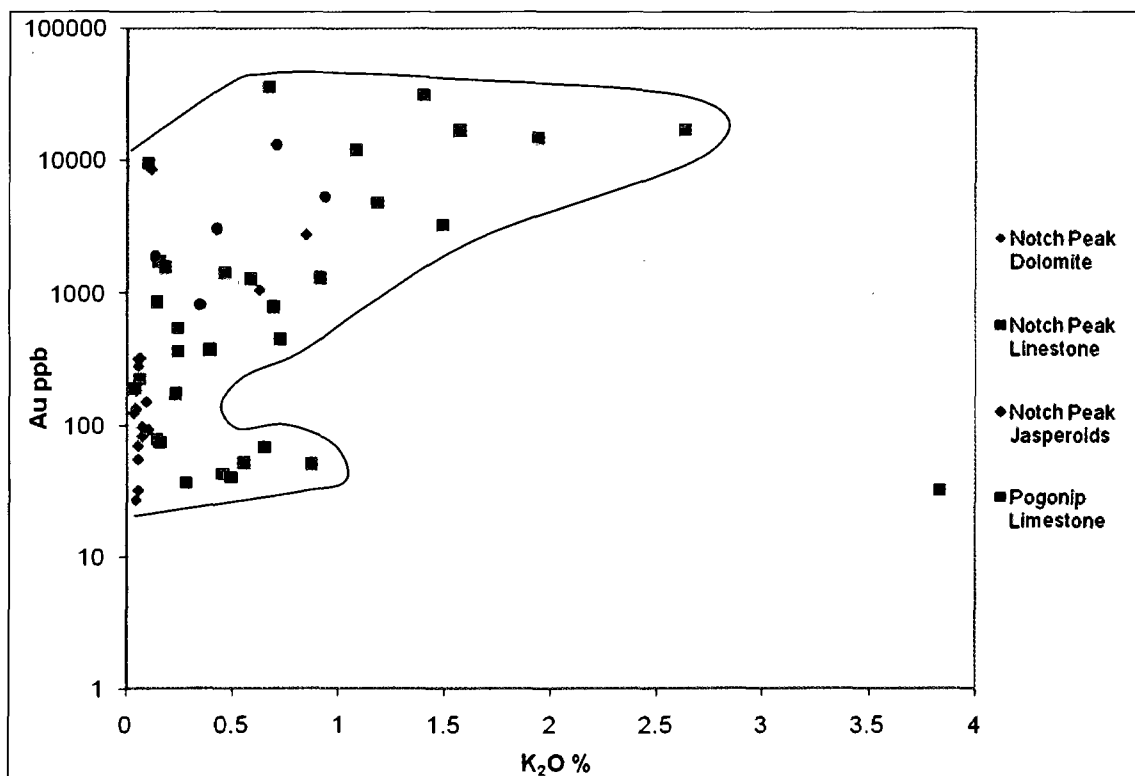


Figure 21. Au vs. K₂O.

Kaolinite

Kaolinite is also indicated in a few carbonate samples. Kaolinite is a prominent component in sample LC07ZJ133, which is a sanded mineralized portion of the Notch Peak dolostone. In thin section sample LC07ZJ133, layers of silt-sized quartz grains along with kaolinite and illite alternate with “layers” of loose dolomite grains. The portion of sample LC07ZJ133 used for making this thin section shows more of a clayey component than is typical (photomicrographs in Appendix A.1). Roughly $\frac{1}{4}$ of the thin section is composed of a clay lens. All other portions of the sample were considered too fragile for sectioning. Generally speaking, kaolinite has a very limited presence in carbonate rocks and it is observed in both strongly mineralized and very poorly mineralized carbonate rocks. As such, its formation is not considered to be a major part of the mineralizing process in carbonate host rocks. Kaolinite is, however, a common alteration product of the intrusive rocks discussed in the following section on intrusions. As can be seen from Table 2, kaolinite occurrences in carbonate rocks are on the whole very minor and occur in both very high and relatively low grade samples.

SAMPLES	Lithology	Au ppb	notes
LC07ZJ069	Pogonip Lst	36080	a faint peak
LC07ZJ165	Pogonip Lst	67	
LC07ZJ167	Pogonip Lst	32	a faint peak
LC07ZJ125	Notch Peak Lst.	14700	a faint peak
LC07ZJ133	Notch Peak Dol.	2778	sanded dolomite, small peak
LC07ZJ037	Intrusive sample	260	
LC07ZJ073	Intrusive sample	124	
LC07ZJ082	Intrusive sample	388	
LLC08ZJ001	Intrusive sample	62	

Table 2. Summary of kaolinite detections in XRD.

Other Minor Mineral Phases

Locally, fine rutile needles have been observed in mineralized and unmineralized carbonate rocks. Observed as fine needles, these rutiles are interpreted as being hydrothermal in origin. Detrital rutile is unlikely to have survived, unbroken, during sedimentary transport. Several but by no means all of the high grade samples in this study have trace rutile. There is some statistical correlation between TiO_2 and Au in the samples examined in this study. This could potentially be due to the presence of trace Ti mixed into the hematite and possibly the original Fe sulfides, associated with gold deposition at Long Canyon and does not necessarily represent a correlation between gold and rutile. Exploration geochemistry does not show any strong correlation between Au and Ti at Long Canyon. It is unclear if these hydrothermal rutile needles have a primary association with Au or if it is merely concentrated in decarbonated rock favorable to Au mineralization. The latter option seems more plausible due to the lack of convincingly strong geochemical association between Au and Ti at Long Canyon.

Apatites were found in both carbonate and intrusive samples, and a detailed description of apatites observed in this study is noted in the following section on intrusive rocks.

In sample L07ZJ081A, a single grain of Cu and Zn alloy was identified in the SEM. It appears to be a cube or flake within a vug in the sample. Initial thoughts were that this occurrence was likely a local contaminant. However, in sample LC07ZJ083, a single grain of Cu:Zn alloy was identified in SEM. Additionally in sample LC07ZJ086 a grain of native Zn was identified by the SEM. Each of these grains has a more natural

appearance (particularly the Cu:Zn grain in LC07ZJ083), lending a greater likelihood that the Cu:Sn grain in sample LC07ZJ081A is not a contaminant (photomicrographs in appendix A.1). The section cutting and polishing process should not incorporate bronze or Cu, Sn, or Zn alloys in the production of petrographic sections. Speculation into the origin of these phases is that they could have resulted from some yet unrecognized source of contamination or that they may be formed by biogenic process after the Au deposition and are not directly related to gold mineralization.

Geochemistry

The results of chemical analysis for samples taken in this study are presented in Appendix B. Tables showing statistical correlations of the chemical constituents within the sample set are shown in Appendix C. Graphs of each element versus gold are shown in Appendix D.1.

Geochemistry of Samples Examined For This Study

Of the Notch Peak dolostone samples, a strong negative correlation is observed between Au and Mg. This shows the affect of decarbonatization in the mineralizing processes. Additionally Al, As, Gd, Hg, La, Mn, P, Sc Si, Sm, Sr, Ti, W, and Y appear to have some correlation to gold. Na also appeared to have a negative correlation to gold in Notch Peak dolostone samples.

Of the Notch Peak limestone samples, strong positive correlation coefficients with Au were observed for Al, As, Be, Cr (as %Cr₂O₃), Fe, Gd, Hg, K (as %K₂O), Na (as %Na₂O), Pb, Sb, Si, Th, Ti (as %TiO₂), V, and Zn. Strong negative correlation coefficients were observed for Ag, Ca, and Li.

There were fewer samples taken from the Pogonip limestone than were taken from the Notch Peak limestones. When those Pogonip limestones are examined independently of the other lithologies, Hg, Sb, and to a lesser extent As, show good correlation with Au. Additionally, Zr shows a strong positive correlation to Au in Pogonip limestones.

The correlation of chemical constituents when examined in all limestone and limestone protolith (excluding Notch Peak dolostone samples) show strong positive correlations of Au to Be, Fe (as %Fe₂O₃), Hg, Li, Pb, Sb, Si (as %SiO₂), Ti (as %TiO₂), and V. Strong negative correlation coefficients were observed for Ag and Ca. Less strong correlations are observed for the other constituents such as As, Al, and Zn.

For the purposes of generating correlation coefficients, jasperoid samples LC07ZJ077, LC07ZJ081A, and LC07ZJ081B were included when analyzing Notch Peak limestones. Also sample LC07ZJ066B was included in the correlation of Notch Peak dolostone samples. Sample LC07ZJ170 was taken in the field from a float sample while its exact protolith is uncertain; it is considered to have been a limestone and as such was included along with samples LC07ZJ077, LC07ZJ081A, and LC07ZJ081B in the correlation of all limestone samples taken from the site. Generally speaking, when these jasperoid samples were excluded from correlation calculations, the resulting correlation coefficients for constituents that show a strong correlation to Au were comparable or slightly stronger than those observed with the jasperoid samples included.

When those samples identified in the field as jasperoids are examined, only Cu has any meaningful correlation to gold. This result is meaningful in that it appears to corroborate the observed presence of trace Cu alloys observed in thin section. Additionally, Ag shows a negative correlation to %SiO₂, and Hg shows a negative correlation to %CaO. The number of samples that were considered jasperoids is limited, but these analyses

suggest that precious metals and associated “Carlin-type” elements are not further enriched by this continued silicification.

In addition to the carbonate samples, the chemistry from the few intrusive samples were also statistically analyzed. The petrography of these samples is discussed in the following section on Intrusive Rocks. Given that these samples are limited and not all the same lithology, statistical analysis of their chemistry should not be expected to reveal much. A positive correlation to Au is observed for Ca and As. The positive correlation between Au and Ca is not unexpected, as some mineralized intrusive samples contain secondary calcite that presumably have replaced plagioclase(?) as part of the alteration process.

Exploration Geochemistry

For the provided exploration rock, soil, and drill chemistry data sets, no attempt was made to segregate samples by lithology before examining the statistical relationships of the various elements to Au. This was due to the inability to personally verify the lithologies of these samples as well as the large size of these data sets, over 1000 samples, each for the rock and soil data sets and over 4000 analysis for the drilling data set. Plots of Au vs. Mg in rock samples and in drill sample data show two distinct populations of data that represent limestone and dolostone samples. All correlations and interpretations of these data must be understood in the context of representing mixed lithologies.

Of the rock samples positive correlations (in these cases, $r > 0.20$) with Au were observed for As, Cd, Hg, Sb, Se, and Tl (The correlation of Se to Au is less strong visually; Appendix D.3). A strong negative correlation between Au and Ca was also observed. Si shows some positive trend with Au when viewed graphically.

Of the drill data, strong positive statistical correlations with Au were observed for As, Cd, Fe, Hg, P, Sb, Sn, Tl, and Zr. A strong negative correlation between Au and Ca was also observed. Si also shows some visible correlation with Au. Graphs of these elements versus gold are presented in Appendix D.4.

Of the soil sample data, strong correlations with gold were observed for As, Hg, and Sb. Graphs of these elements versus gold are presented in Appendix D.2.

A location map of all rock and soil samples discussed here is provided on Plate 4 to give context to the statistical and well as spatial observations made in this study. Contours of Au, As, Sb, and Hg, values for the soil grid shown on Plate 4 are presented in Plates 5 a., 5 b., 5 c., and 5 d. The anomalies for As, Sb and Hg all concentrate around and extend outside the gold anomaly. All elements presented here show some degree of down slope transport from a source or areas of high concentration, Sb in particular. Areas of high As, Sb, and Hg concentrations that do not conform to observed Au anomalies could represent locations of unexposed Au mineralization, particularly where associated with lithologic contacts between limestone and dolostone units. As and Sb anomalies in the NW corner of each plate should be understood to be outside of the soil grid on Plate 4. These and

other anomalies outside the soil grid are a result of the kriging process and do not necessarily represent a true geochemical anomaly.

Intrusive Rocks

Altered intrusive rocks are locally found in Notch Peak and Pogonip limestone units and as float in numerous places in the study area. Mineralized and unmineralized samples of intrusive rocks were collected from float and road cuts in the study area. Figure 22 is a chondrite normalized plot of trace element geochemistry from intrusives sampled at Long Canyon. Figures 23 through 28 illustrate the textural and mineralogical features of the sampled intrusives.

Intrusives sampled in this study fall into two categories. The first type is represented by sample LC07ZJ065 (Au= 92ppb). It is a calc-alkaline lamprophyre. In hand sample it is a green, propylitic, medium grained intrusive. The proportion of light to dark minerals is roughly equal with average grain sizes of ≈ 0.5 mm. In thin section, panidiomorphic phenocrysts of hornblende dominate, comprising 50% of the sample volume. Oligoclase is the primary matrix material comprising 33% of the sample. Roughly 5% of the sample is quartz. There is observable micrographic texture present in interstitial quartz and feldspar, commonly as epitaxial overgrowths on feldspar. Elongate apatite crystals comprise as much as 1% of the sample by volume. Additional phases include trace amounts of allanite (Ce), trace Fe oxide pseudomorphs of pyrite, and abundant sericite. Conspicuously absent is olivine, as it was both expected in hand sample and is a common (but not essential) lamprophyre mineral.

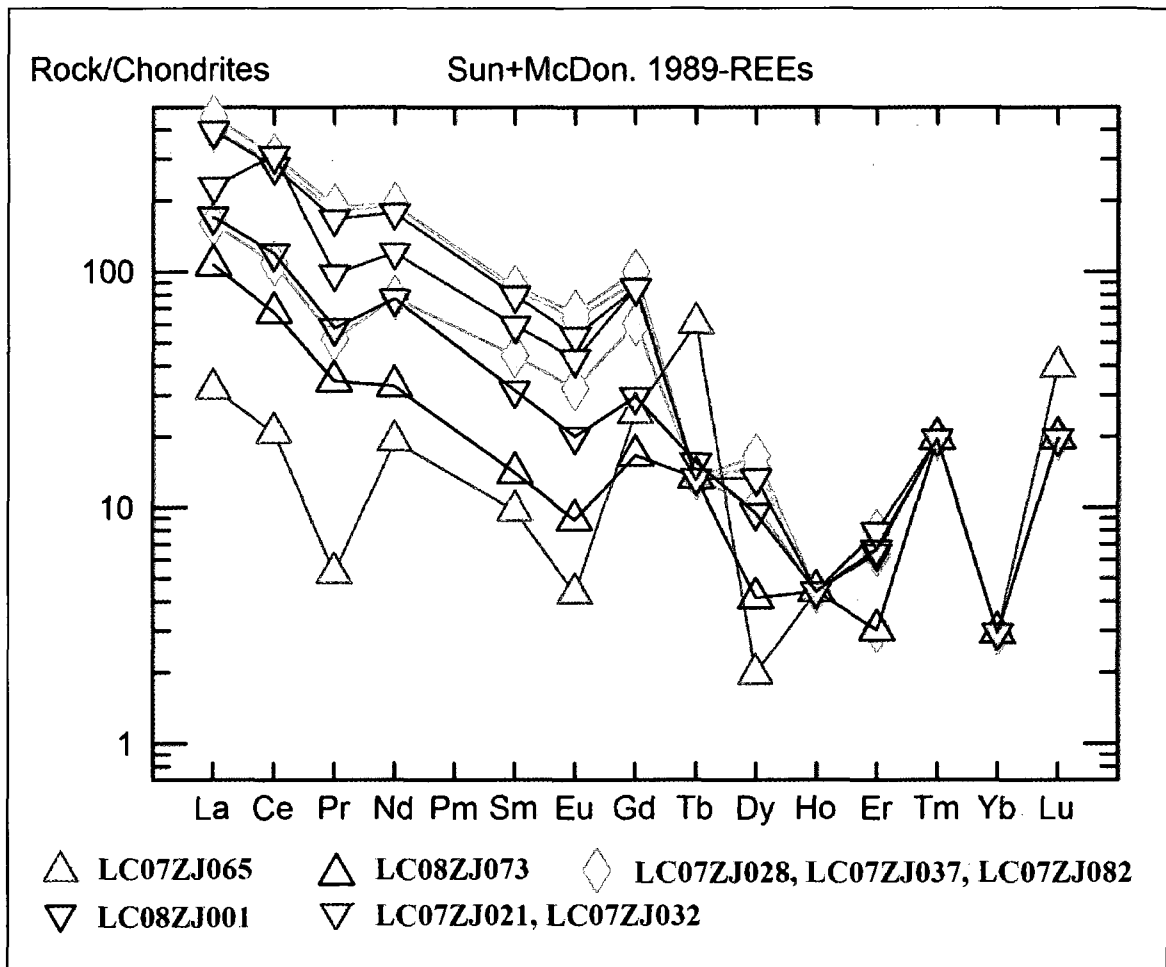


Figure 22. Chondrite normalized plot diagram for rare earth elements in Long Canyon intrusive rocks. The figure shows a negative europium anomaly for each sample. Eu can substitute for Ca in plagioclase. The depletion of Eu in relation to other rare earth elements indicates that plagioclase crystallized early and settled in the magma chamber increasing the mafic content of the magma prior to intrusion. The overlapping data points for Ho, Tm, Yb, and Lu values represent concentrations found to be below analytical detection limits. The chemical concentrations for these data were set at a value equal to one half the analytical detection limit.

Table 3 compares the results of whole rock geochemistry to those of typical lamprophyres as published by Rock (1987). The sample chemistry of LC07ZJ065 is similar to both alkaline and calc-alkaline lamprophyres; however the presence of primary quartz precludes its classification as an alkaline lamprophyre (Rock, 1991 p. 41). In addition to its mineralogical differences, this sample can be seen to have a distinctly different trace element geochemical signature on the chondrite normalized plot (Fig. 22)

related to other intrusive samples taken from Long Canyon. The mineralogical and chemical data allow this intrusion to be classified as a hornblende rich calc-alkaline lamprophyre.

	SiO ₂	Al ₂ O ₃	CaO	MgO	Na ₂ O	K ₂ O
LC07ZJ065	52.38	15.11	7.74	6.70	2.84	1.48
LC08ZJ001	34.35	18.03	1.60	17.54	0.01	2.69
CAL	46-57	11-18	4-9	3-10	1.5-4	3-7
AL	36-46	10-16	7-15	4-10	2-5	1-3
UML	20-35	2-12	10-20	8-20	0-3	1-3

Table 3. Analytical results for unmineralized intrusive rocks collected at Long Canyon compared to typical whole rock oxide ranges for calc-alkaline(CAL), alkaline (AL) and ultra-mafic (UML) lamprophyres provided by Rock (1991, p. 41).

The second type of intrusion sampled at Long Canyon is best represented by sample LC08ZJ001 (Au= 62ppb). It is an unmineralized, though altered, mafic to intermediate intrusive previously thought to be a lamprophyre. Its similarities and differences from lamprophyric rocks are discussed below. While the alteration of the samples available makes a clear and definite classification of these intrusive rocks uncertain, for purposes of this study they are tentatively classified as being quartz monzodiorite. It was sampled from a road cut, where it is hosted in unmineralized Pogonip limestone and is oriented parallel or near parallel to bedding. In hand sample and cut slab, it consists of fine panidiomorphic biotite crystals generally no larger than 1mm in size. Biotites appear to have preferred orientation giving the rock a foliated look. The sample also contains hematite pseudomorphs after pyrite. Fe oxide streaks are visible along foliation planes. In thin section the sample is composed of platy, <0.5 mm biotites that make up \approx 20% of the sample by volume. SEM analysis suggests the biotite contains Ti in addition to Mg and Fe. The matrix is fine albite and lesser quartz with other optically unidentifiable phases. Apatite needles are also present. Minerals not observed in thin section but

indicated in the samples X-ray diffraction pattern include: spinel, vermiculite, and kaolinite. As can be seen in Table 3, the whole rock chemistry for sample LC08ZJ001 is not consistent with any one type of lamprophyre (nor is it consistent with similar intrusive rocks such as lamproites) but bears some similarities to all three lamprophyre groups. The high silica content and the presence of quartz in the sample is most likely a result of alteration, as opposed to sample LC07ZJ065, a different intrusive phase that contains primary quartz. If any quartz were primary to sample LC08ZJ001, it would preclude classifying the sample as an “ultramafic” type lamprophyre (Rock, 1991, p. 41).

Further the chondrite normalized plot presented as Figure 22 shows a relationship between samples LC08ZJ001 and LC07ZJ82. Figures 25 and 26 show in sample LC07ZJ082 a plagioclase(?) phenocryst that has been replaced by calcite. A lamprophyre by definition should have no feldspar phenocrysts. There is ample mineralogical and textural evidence to suggest that samples LC07ZJ021 and LC07ZJ032 as well as those of the argillized intrusives sampled as float were mineralogically similar to LC08ZJ001 and are likely the same or a related intrusive phase. This will be discussed in more detail in the following section on alteration.

Sample LC07ZJ073 is a highly altered (argillized) seemingly aplitic intrusive sampled from float on the ridge top between Long Canyon and the study area. It is primarily composed of kaolinite, sericite and quartz. The sample's original mineralogy and texture are obscured by clay alteration (kaolinite). Pyrite is present and has largely been replaced by Fe-oxide pseudomorphs. Rare rhombohedral carbonate grains are also present. The

sample is low grade (Au = 124 ppb) and physically bears little resemblance to any of the other intrusions sampled on the site. However, on the chondrite normalized plot (Fig. 22) presented below, there is a chemical similarity between this sample and other intrusive samples at Long Canyon. As such, it is at this time loosely grouped with the other intrusives, other than sample LC07ZJ069.

Alteration and Mineralization

Samples LC07ZJ021 and LC07ZJ032 were taken from a sericitically altered and mineralized intrusive dike swarm found intruding unmineralized Notch Peak limestone in an exposed road cut. The samples are characterized as being strongly hematitic. Hematite is present as disseminated oxide and as anhedral pseudomorphs after pyrite. Disseminated Fe-oxide is particularly concentrated in the pseudomorphs of biotites that have been completely replaced by illite. Apatites are commonly observed in quartz. Each sample also contains trace amounts of aluminum chromite. Sample LC07ZJ032, assayed at 26 ppm Au, is the highest grade of all intrusive rocks sampled. Samples LC07ZJ037 and LC07ZJ082 are float samples of argillized intrusive rocks, and they have been altered to clays and oxides. X-ray diffraction patterns for these two samples indicate common alteration products of kaolinite, illite, hematite, quartz, and calcite. In sample LC07ZJ082, calcite is locally seen completely replacing feldspar(?) phenocrysts. Sample LC07ZJ028 is sericitically altered. It shows some petrographic evidence of clay replacement of silicate minerals however no clay minerals, such as kaolinite, show up in XRD analysis. Instead the X-ray diffraction pattern for sample LC07ZJ028 shows muscovite, hematite, and quartz.

Summary and Discussion of Igneous Rocks

Samples LC07ZJ021, LC07ZJ028, LC07ZJ032, LC07ZJ037, and LC07ZJ082 all contain textural and/or mineralogical similarities to sample LC08ZJ001 which is tentatively classified as a quartz monzodiorite. The chief textural similarity with sample LC07ZJ001 is that the mineralized intrusives have platy biotite. This textural similarity is best observed in samples LC07ZJ021 and LC07032, in which biotite has been completely replaced by illite and is strongly coated with hematite preserving the platy structure of biotite. Aluminum chromite is visible in thin sections LC07ZJ021, LC07ZJ032, and LC07ZJ082. Chromite is a spinel group mineral, and spinel is indicated in the X-ray diffraction pattern for LC08ZJ001, though no spinel group minerals are optically identifiable in thin section. Sample LC07ZJ065 is texturally, mineralogically and chemically distinct from the other intrusive rock samples examined in this study. It is classified as a propylitically altered, hornblende rich, calc-alkaline lamprophyre.

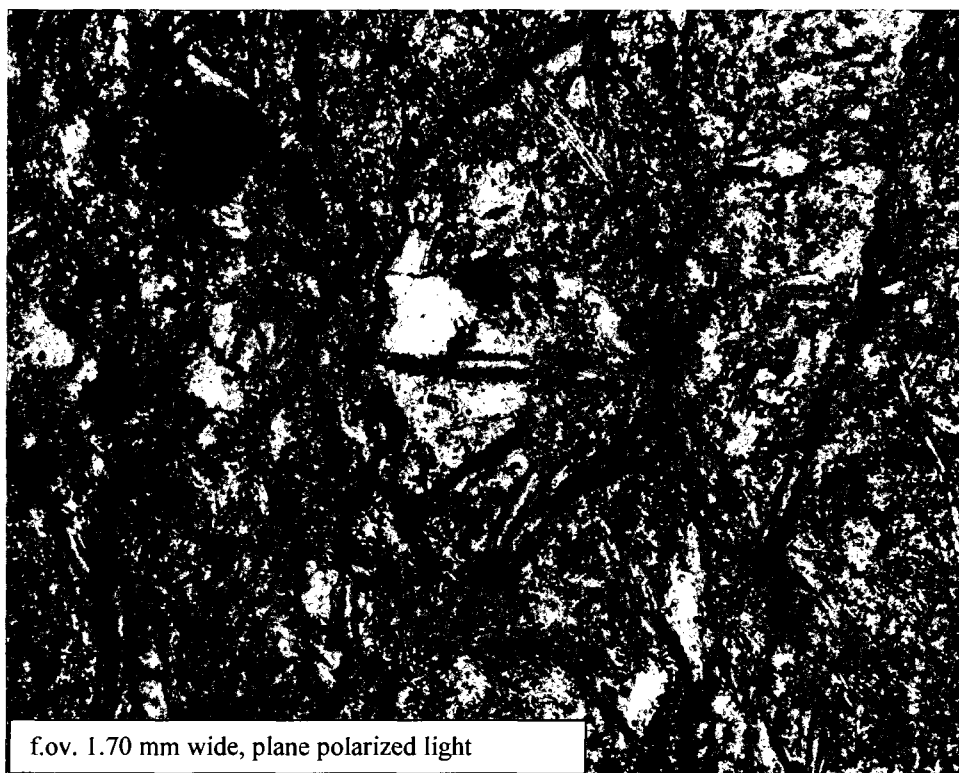


Figure 23. LC08ZJ001: Platy biotite in matrix of albite and quartz.

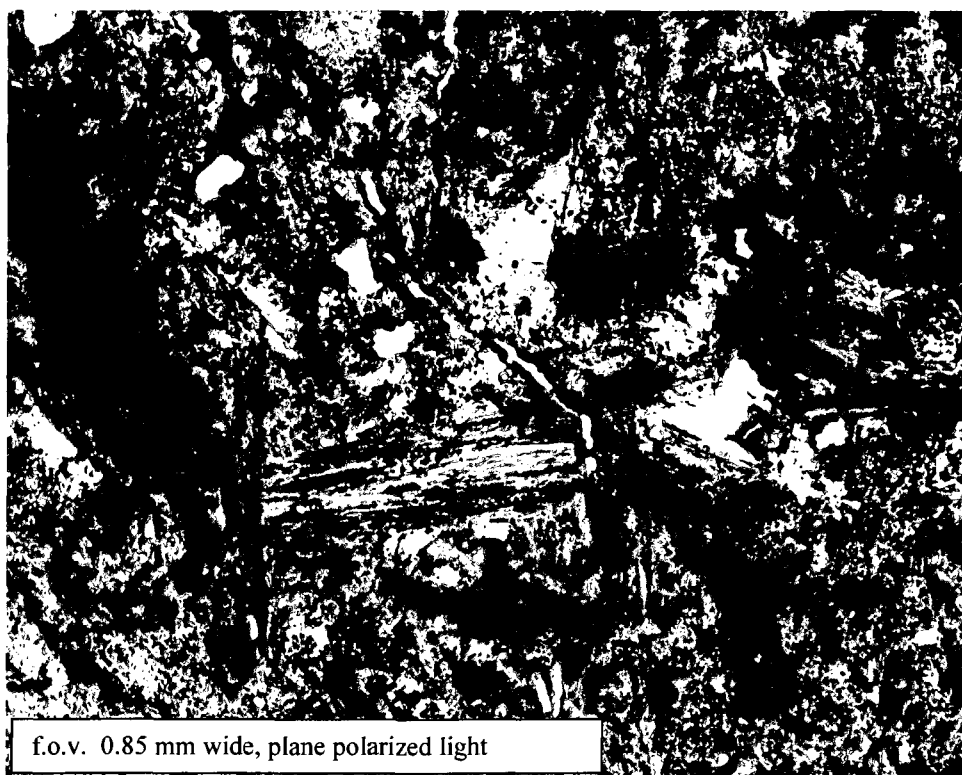


Figure 24. LC07ZJ032: Platy biotite replaced by illite and hematite.

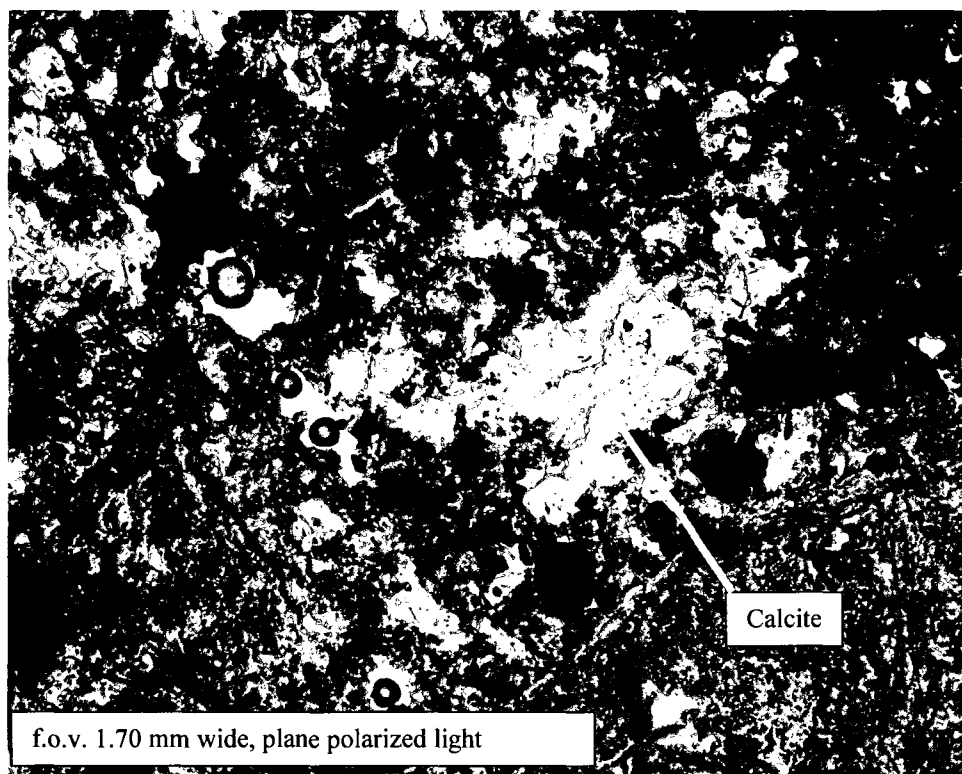


Figure 25. LC07ZJ082: calcite replacement of feldspar(?) phenocryst.

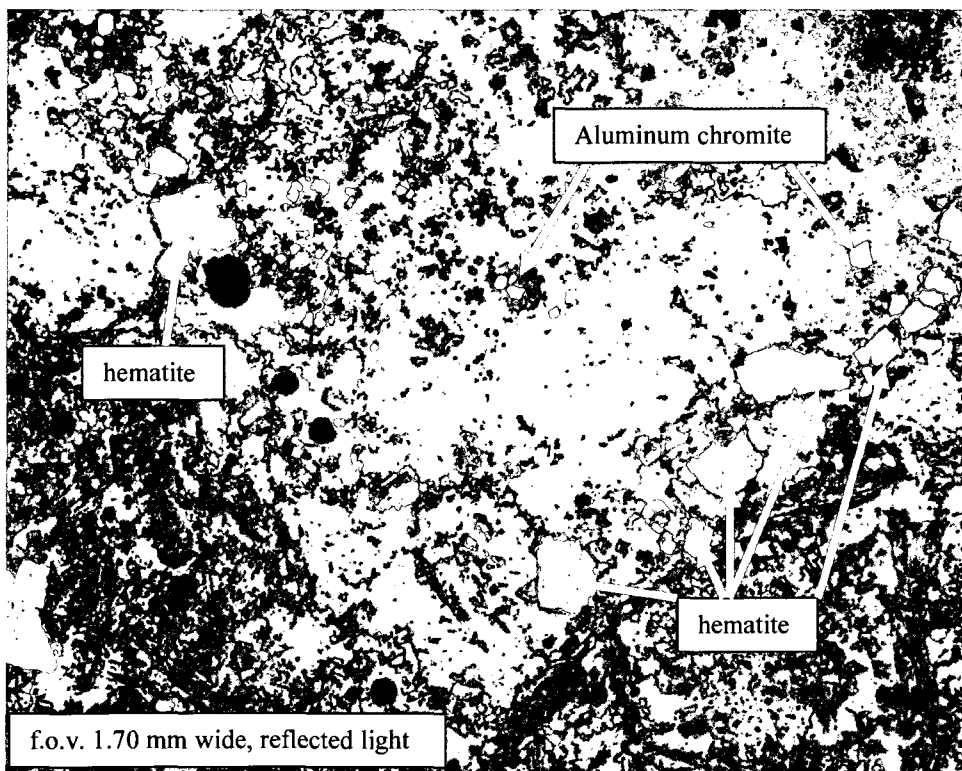


Figure 26. LC07ZJ082: same view as Figure 25, in reflected light.

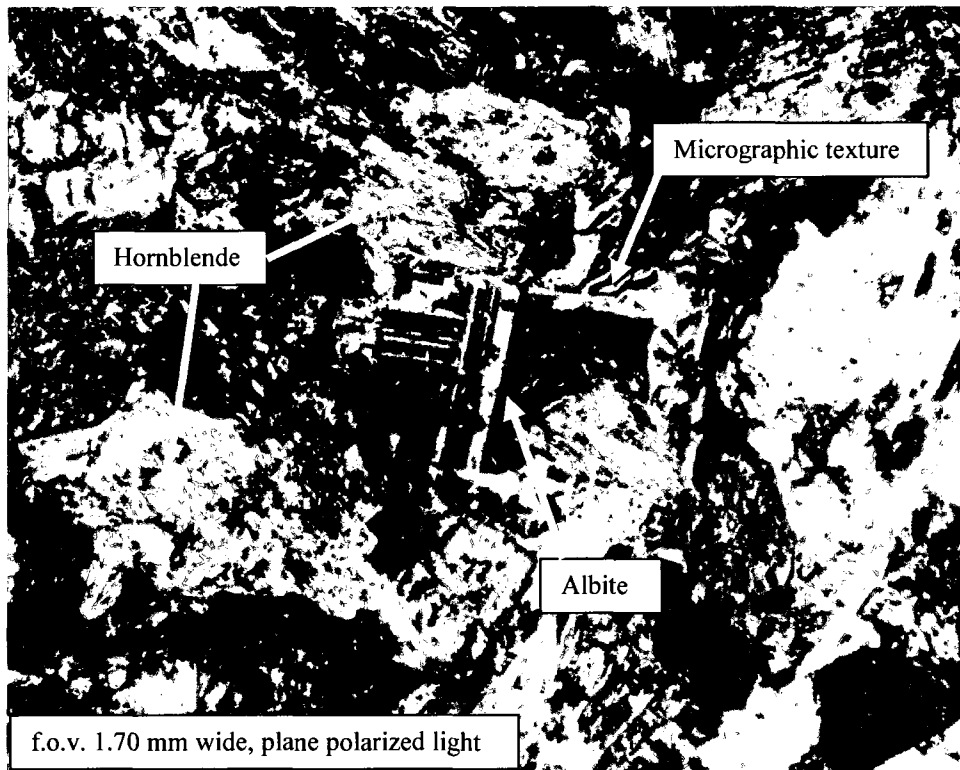


Figure 27. LC07ZJ065: Hornblende with plagioclase (twinned). Few good albite twins were observable. Measurements of those few albite twins (Michel-Levy Method) show a highest average extinction angle $\approx 10-10.5^\circ$ in biaxial (-) plag: An_{16} (Oligoclase).

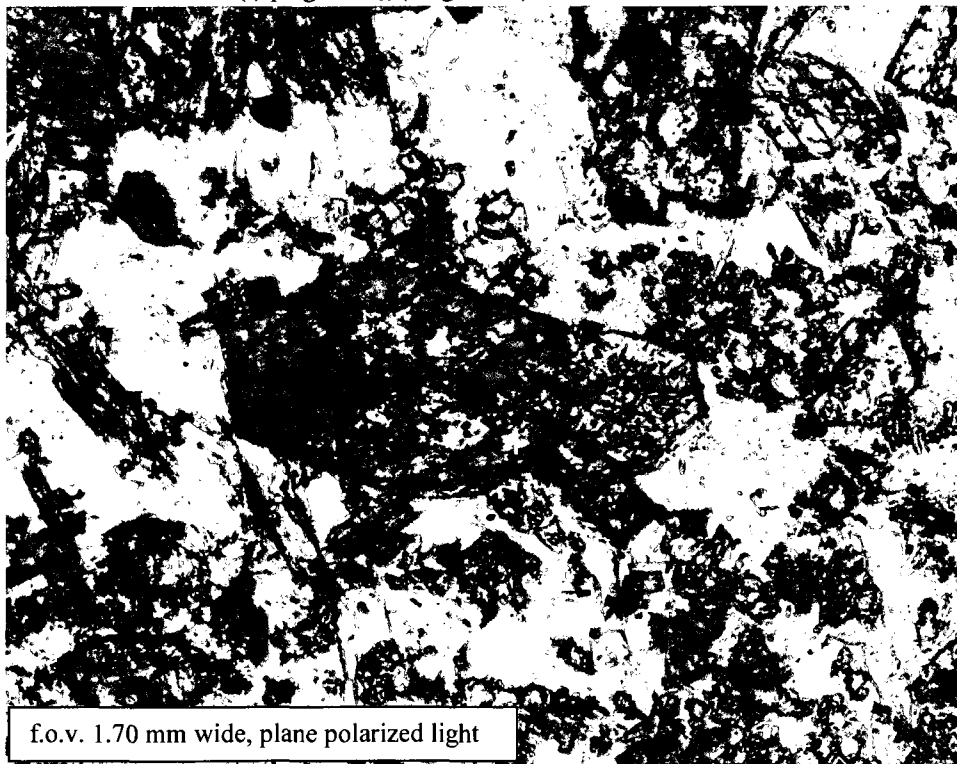


Figure 28. LC07ZJ065: Hornblende altering to chlorite; Allanite (Ce) fan; Apatite needles in Oligoclase.

Apatite

In total, 17 samples were found to contain apatite. A summary of those occurrences is presented in Table 4. Apatites are commonly observed in intrusive samples as well as in samples of Notch Peak dolostone, and are locally found in limestone samples as well. A correlation between phosphorus to gold is indicated from Fronteer drill data and to a lesser degree in the surface rock sample data set. Additionally, samples for Notch Peak dolostone examined in this study showed a weak statistical correlation between P and Au.

Apatites range in color from clear with a slight green tint to strongly green in color and have euhedral form. In intrusive rocks, apatite crystals tend to be slender needles with lengths up to $\frac{1}{4}$ mm. In those samples that have been strongly mineralized, apatite is seen entirely encapsulated in silica. In unmineralized intrusions, apatite can be observed within silica as well as in the feldspar matrix.

In contrast, apatite crystals observed in carbonate rocks have shorter, commonly stubby, crystal forms. In carbonate samples, apatite is always observed encapsulated in secondary or recrystallized quartz (Fig. 29).

Preliminary observations indicated that the apatites present within this sample set could prove useful in dating alteration. However after the completion of petrographic observations, it was determined that the available apatite crystals in this sample set were insufficient in size and quality to effectively attempt fission track dating.

Lithology	Sample	Au ppb	Visual I.D. Thin Section	XRD Fluorapatite Ca ₅ (PO ₄) ₃ F	P ₂ O ₅ %	SiO ₂ %	P ppm
Notch Peak Dol.	LC07ZJ001	83	X		0.07	2.54	215
Notch Peak Dol.	LC07ZJ101	326	X		0.13	1.38	403
Notch Peak Dol.	LC07ZJ103	124	X		0.12	2.31	502
Notch Peak Dol.	LC07ZJ107	1063	X		0.30	46.04	858
Notch Peak Dol.	LC07ZJ133	2778	X	X	0.45	46.61	1860
Notch Peak Dol.	LC07ZJ148	98	X		0.11	3.44	395
Notch Peak Lst.	LC07ZJ124	1721	X		0.19	7.63	666
Notch Peak Lst.	LC07ZJ153	16810	X	X	0.03	83.18	176
Pogonip Lst.	LC07ZJ022	40		X	0.15	25.27	440
Pogonip Lst.	LC07ZJ069	36080		X	0.75	64.84	2890
Intrusive sample	LC07ZJ021	868	X	X	0.96	55.94	3710
Intrusive sample	LC07ZJ028	542		X	0.94	59.39	4600
Intrusive sample	LC07ZJ032	24800	X		0.76	38.67	4580
Intrusive sample	LC07ZJ037	260	X	X	1.16	55.30	2990
Intrusive sample	LC07ZJ065	92	X	X	0.20	52.33	860
Intrusive sample	LC07ZJ082	388	X	X	0.91	51.78	3260
Intrusive sample	LC08ZJ001	62	X	X	1.02	34.06	3250

Table 4. Summary of apatite in sample set.

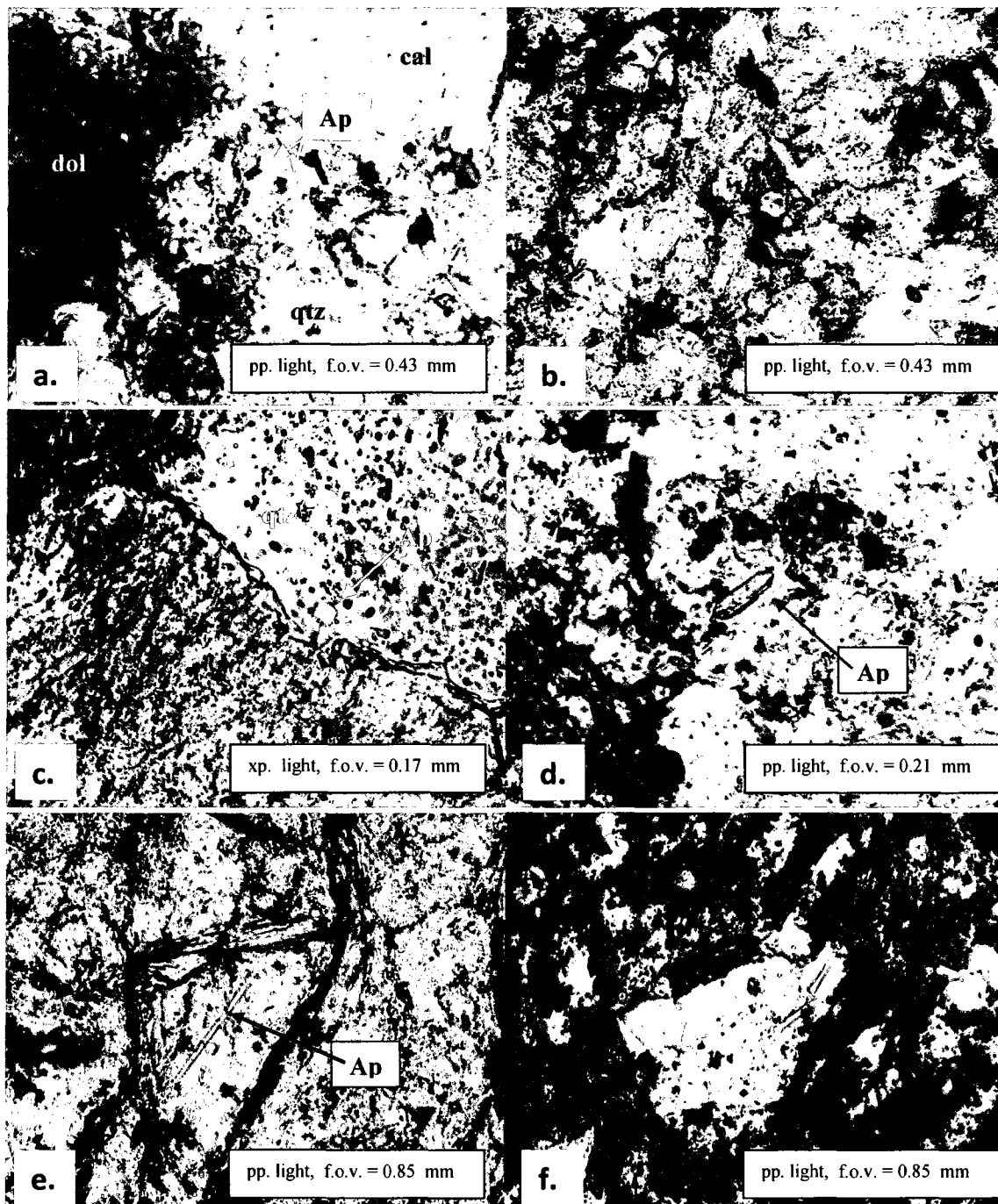


Figure 29. a.) LC07ZJ101: Fine euhedral apatite in secondary quartz in Notch Peak dolostone. b.) LC07ZJ153, very small apatite encapsulated in the hexagonal quartz crystal in the center of the image of sanded Notch Peak limestone. c. and d.) LC07ZJ103 and LC07ZJ133 apatites in secondary quartz in Notch Peak dolostone. e.) apatite needle in albitic matrix of sample LC08ZJ001. f.) apatite needles in quartz, mineralized intrusive sample LC07ZJ021.

Discussion

Arehart *et al.* (1993), following early work by Wells and Mullans (1973) established that in the Carlin-type deposits of Nevada, gold precipitates with arsenian pyrite, particularly when forming as rims on preexisting nonarsenian, non-auriferous pyrite. This feature is considered to be a defining characteristic of Carlin-type disseminated gold deposits. In this study, the presence of arsenian pyrite forming as rims on non-arsenian pyrite has been demonstrated. Additionally, in one sample (LC07ZJ156), gold has been shown to have some spatial relation to pyrite rims. All other optically identifiable gold occurrences observed in this study are free blebs with no close relation to pyrite or Fe oxide pseudomorphs after pyrite. It is possible that this could represent remobilization of gold under later alteration and oxidation of the host rock. The gold grains observed in this study are relatively free of silver. This suggests that they may have formed under oxidized conditions, in which silver would have been dissolved.

Mineralization at Long Canyon displays other typical Carlin-type features. Chemical and petrographic evidence show the importance of decarbonatization and silicification in relation to gold at Long Canyon. Mineralized limestones have much larger silica content than is readily observable at the outcrop and hand sample scale. Silica grains in decarbonatized limestones are commonly anhedral or irregular in shape, but they can also show euhedral features such as doubly terminated crystals, suggesting crystal growth of grains with carbonate dissolution. While some of the silica certainly originates from the silty components in limestone, most of the silica in ore zones is introduced. Introduced silica forms either as overgrowths of preexisting quartz grains or as infilling of void

spaces in carbonate host rocks. Silica input to the system, while considerable, was insufficient to produce massive wide-spread exposures of silicified rock or jasperoid.

The host rocks at Long Canyon are strongly oxidized. Sulfide minerals are only observed where they are encapsulated in quartz and locally in carbonate. Fe shows both a chemical relation to gold and a strong visual relation is observed as high Au grade samples tend to be visibly hematitic. In mineralized carbonate samples, Fe oxide either as pseudomorphs after pyrite or as disseminated Fe oxide are common. Additionally, local jarosite and scorodite have been related to high-grade mineralization in carbonate samples. Non-mineralized carbonate rocks at Long Canyon are also strongly oxidized with Fe oxide occurring as both pseudomorphs after pyrite or as disseminated Fe oxide, which is generally composed of varying degrees of hematite and goethite. In mineralized intrusive samples, hematite also forms as pseudomorphs after pyrite or as disseminations that can be found as a thick coatings on illite pseudomorphs after biotite.

Argillization does not appear to play any substantial role in alteration of carbonate host rocks. However argillization is apparent in several of the intrusive rocks locally present at Long Canyon. Those dikes that carried significant gold grades tend to be strongly sericitic (or illitic) rather than argillized, though locally kaolinite is present in some mineralized intrusive rock samples. The presence of intrusions like those observed at Long Canyon also represents a similarity to other known Carlin-type deposits in Nevada. Typical of Carlin-type systems, As, Sb, Hg Si, Fe, and Tl all show strong correlation with Au. At Long Canyon, Sb and Hg show a particularly strong association with Au. Soil

anomalies for Au, As, Sb, and Hg generated for the study area show a broadly NE-SW orientation. High geochemical signatures tend to be localized along limestone-dolostone boundaries. Exploration geologists working at Long Canyon have produced a unique model for the structural control of mineralization at the site.

Conclusions and Areas of Future Research

Gold mineralization at Long Canyon can be classified as being Carlin-type. This is based on the presence of characteristic rims of arsenian pyrite observed as overgrowths of preexisting pyrite. Additionally the association of gold to typical Carlin-type elements namely As, Sb, Hg Si, Fe, and Tl also points to mineralization being Carlin-type in nature.

The mineralogical interpretations made here are from surface samples only. Examination of subsurface sample mineralogy and alteration will no doubt add to the understanding of the project. Further investigation into apatite mineralogy in both carbonate as well as intrusive rocks may aid in establishing a date for mineralization at Long Canyon.

Ongoing exploration

At the time sampling was ongoing for this project, drilling had yet to be initiated south of the line of 4538100 meters North. Given the strong concentrations of Au, As, Sb, and Hg associated with limestone-dolostone contacts immediately to the south of that line, it should be expected that drilling in this area will likely discover economically viable ore zones as have already been identified to the north. Drilling in this area was planned for

the summer field season of 2009. Since the initiation of this study, exploration has progressed north and northeast of the thesis study area. These exploration efforts have been fruitful, adding to the overall known volume of possible minable gold at Long Canyon. AuEx Ventures Inc. reported in a March 13, 2009, press release that as of February 9, 2009, Long Canyon has an indicated resource of 363,000 ounces of gold at an average grade of 2.35 g/t gold and an inferred resource of 459,000 ounces of gold at an average grade of 1.63 g/t. These resource estimates were made with a cutoff grade of 0.3 g/t gold. (www.auexventures.com). At the time of the writing of this thesis, ore zones are considered to still be “open” both to the north and to the south, and ongoing exploration is planned for the site (www.frontiergroup.com).

References Cited

- Archart, G. B., Chyssoulis, Stephen L., Kesler, and Stephen E., 1993, Gold and arsenic in iron sulfides from sediment-hosted disseminated gold deposits: Implications for depositional processes: *Economic Geology*, v.88, p. 171-185.
- Camilleri, Phyllis A., 1994, Mesozoic and Cenozoic tectonic and metamorphic evolution of the Wood Hills and Pequop Mountains, Elko County Nevada: (Thesis) University of Wyoming, 390 p.
- _____, P. A., and Chamberlain Kevin R., 1997, Mesozoic tectonics and metamorphism in the Pequop Mountains and Wood Hills reagon, northeast Nevada: Implications for architecture and evolution of the Sevier Orogen: *Geological Society of America Bulletin*, January 1997, p. 74-94.
- Cline, J. S., Hofstra, A. H., Muntean, J. L., Tosdal, R. M., and Hickey, K. A., 2005, Carlin-Type Gold Deposits in Nevada: Critical Geologic Characteristics and Variable Models: *Economic Geology*, 100th Anniversary Volume, p. 451-484.
- Hintze, L. F., M. E. Taylor, and J. F. Miller. 1988, Upper Cambrian– Lower Ordovician Notch Peak Formation in western Utah. *United States Geological Survey Professional Paper 1393*, 30 p.
- McCollum, Linda B., and Miller, David M., 1991, Cambrian Stratigraphy of the Wendover Area, Utah and Nevada: *U.S. Geological Survey Bulletin 1948*, 43 p.
- Miller, J. F., K. R. Evans, J. D. Loch, R. L. Ethington, and J. H. Stitt., 2001, New lithostratigraphic units in the Notch Peak and House formations (Cambrian– Ordovician), IbeX area, western Millard County, Utah: *Brigham Young University Geology Studies*. v.46, p. 35–69.
- Nolan, T.B., Merriam, W. C., Williams, J. S., 1956, The Stratigraphic Section in the Vicinty of Eureka, Nevada: *U.S. Geological Survey Professional Paper 267*, 77 p.
- Rock, N. M. S., 1991, Lamprophyres [by N.M.S. Rock], with additional invited contributions from D. R. Bowes and A. E. Wright, 285 p.
- Smith, Moira, 2009a, Summary of geology and presentation of a geological model for Long Canyon, with emphasis on field surveys, Fronteer Development USA Inc. unpublished, internal company report, 98 p.
- _____, 2009b, personal communication.

- Thorman, C. H., 1962, Structure and stratigraphy of the Wood Hills and a portion of the northern Pequop Mountains., Elko Co., Nev.: (Thesis) University of Washington, 218 p.
- Thorman, C. H., 1970, Metamorphosed and nonmetamorphosed Paleozoic rocks in the Wood Hills and Pequop Mountains, Northeast Nevada: Geologic Society of America Bulletin, v. 81, p. 2417-2448.
- Thorman, C. H., Ketner, K. B., Brooks, W.E., Peterson, F., 1992, Elko Orogeny in Northeastern Nevada; Structural geology and petroleum potential of southwest Elko County, Nevada: the guidebook to the Nevada Petroleum Society annual field trip, June, 1992. p. 1-3.
- Thorson, J. P., 2007, RE – Long Long Canyon project: unpublished, internal report made to New West Gold Corporation, 31 p.
- Walcott, C. D., 1908a, Nomenclature of some Cambrian Cordilleran Formations: Smithsonian Miscellaneous Geological Collections, v. 53, no. 1, p. 1-12.
- _____, C. D., 1908b, Cambrian Section of the Cordilleran area: Smithsonian Miscellaneous Geological Collections, v. 53, no. 5, p. 167-230.
- Wells, J. D., and Mullens T.E., 1973, Gold-bearing arsenian pyrite determined by microprobe analysis, Cortez and Carlin gold mines, Nevada: Economic Geology, v. 68, p. 183-201.